Expression pattern, tumor immune landscape, and prognostic value of N7-methylguanosine regulators in bladder urothelial carcinoma

CHI ZHANG[1*], JIANGNAN XIA[2*], SIMIAO ZHANG[3], JING LI[4], TIAN ZHOU[1] and KAIWEN HU[1]

[1]Department of Oncology, Dongfang Hospital, Beijing University of Chinese Medicine, Beijing 100078; [2]School of Basic Medical Sciences, Guangzhou University of Chinese Medicine, Guangzhou, Guangdong 510006; [3]School of Chinese Medicine, Hunan University of Chinese Medicine, Changsha, Hunan 410208; [4]Department of Oncology, The First Hospital of Hunan University of Chinese Medicine, Changsha, Hunan 410021, P.R. China

Received November 4, 2022; Accepted February 17, 2023

DOI: 10.3892/ol.2023.13755

Abstract. N7-Methylguanosine (m7G) modification is important in post-transcriptional regulation. dysregulation of m7G RNA modification has been reported to be markedly associated with cancer. However, its importance in bladder urothelial carcinoma (BLCA) remains poorly characterized. The present study systematically analyzed mRNA gene expression data and clinical information from The Cancer Genome Atlas and further constructed robust risk signatures for the four regulators of m7G RNA modification (nudix hydrolase 11, gem nuclear organelle-associated protein 5, eukaryotic translation initiation factor 3 subunit D and cytoplasmic FMR1 interacting protein 1). The differential expression and cell function of m7G-related genes in bladder cancer cells were verified by reverse transcription-quantitative PCR, Cell Counting Kit-8 and colony formation assays. The four-gene-based model could accurately predict the prognosis of BLCA. Nomogram-based clinical decisions had a higher net benefit compared with that of individual predictors. Through immune infiltration analysis, it was found that immune cell infiltration affected the prognosis of patients with BLCA. Finally, the present study identified potential therapeutics that differ between high and low-risk groups based on four genes. In summary, the current findings revealed an essential role for m7G RNA modification regulators in BLCA, and developed risk signatures as promising prognostic markers in patients with BLCA.

Correspondence to: Dr Kaiwen Hu, Department of Oncology, Dongfang Hospital, Beijing University of Chinese Medicine, 6 Fangxingyuan, Fengtai, Beijing 100078, P.R. China
E-mail: kaiwenh@163.com

*Contributed equally

Abbreviations: BLCA, bladder urothelial carcinoma; GEMIN5, gem nuclear organelle-associated protein 5; CYFIP1, cytoplasmic FMR1 interacting protein 1; NUDT11, nudix hydrolase 11; EIF3D, eukaryotic translation initiation factor 3 subunit D; PD-1, programmed cell death 1; PD-L1, programmed cell death ligand 1; CTLA4, cytotoxic T lymphocyte-associated protein 4; ROC, receiver operating characteristic

Key words: bladder cancer, prognostic model, bioinformatics, immune infiltration, N7-methyladenosine

Introduction

Bladder urothelial carcinoma (BLCA) is a malignant tumor of the bladder urothelium accounting for ~500,000 new cases and 200,000 mortalities worldwide each year (1). Approximately 70% of patients with BLCA have non-muscle-invasive bladder cancer (NMIBC), and usually undergo transurethral resection of the bladder tumor and subsequent radiotherapy, chemotherapy, or immunotherapy. However, ~80% of patients suffer NMIBC recurrence within 5 years of diagnosis, with tumor progression occurring in 30% of cases (2). For these patients, a combination of surgery, radiotherapy, chemotherapy, and immunotherapy can be used (3). However, these treatments increase the surgical risk and treatment-related toxicity, and patients with aggressive or advanced BLCA still face adverse clinical outcomes. A remaining challenge is designing approaches to filter patients who may benefit from aggressive treatment. Therefore, novel biomarkers that can be used to predict prognosis and treatment response are urgently needed.

Bioinformatics has become an integral tool in biomedical research and treatment development in the past decade, and it plays a vital role in deciphering genomes, transcriptomes, and proteomes generated via high-throughput experimental techniques or from tissues collected in traditional biological studies (4). For example, sequence-based methods used to analyze multiple genes or proteins have been explored (5). The primary purpose of bioinformatics analysis is to mine the association between features according to the feature information based on multidimensional data. Based on public databases, potential associations among clinical patient parameters are analyzed, and this can be used to the reveal risk factors of a disease, further develop survival prediction models for a disease, and develop precise diagnoses and

treatment recommendations for patients (6). Through bioinformatics analysis, previous studies have identified molecules and phenotypes associated with the diagnosis, treatment, and prognosis of BLCA, such as pyroptosis (7), immune cell infiltration (8-10), hypoxia (11), and inflammation (12). However, several other biological features of BLCA remain to be identified.

The recent progress made in the understanding of epitranscriptomics has led to the identification of numerous types of post-transcriptional modifications of eukaryotic RNA, such as 5-methylcytosine, N6-methyladenosine, and N7-methylguanine (m7G) (13). Methylated m7G RNA is one of the most conserved modified nucleosides, and is commonly detected in eubacteria, eukaryotes, (14) and archaea (15). m7G modification, which adds a methyl group to the seventh N of guanine (G) in RNA via a methyltransferase, is an important form of base modification involved in post-transcriptional regulation. Recently, m7G-related genes have attracted widespread attention in oncology; for example, a previous study has shown that methyltransferase 1 (METTL1)-mediated m7G transfer RNA (tRNA) modification can boost oncogene translation and promote the progression of intrahepatic cholangiocarcinoma (16). Based on the association between tumors and m7G, a previous study identified six genes associated with poor patient prognosis, thus showing potential for evaluating gastric cancer prognosis (17). However, to the best of our knowledge, there are no studies that have investigated the expression pattern, molecular function, or prognostic value of m7G-related regulatory genes in BLCA; thus, the present study aimed to mine the differentially expressed genes between BLCA samples and normal healthy tissues and to construct a prognostic model to explore the potential function of m7G in this disease. Furthermore, with the increasing use of immunotherapy and personalized medicine, immune infiltration has become a prognostic factor for multiple cancer types, and thus, the present study further predicted the immune landscape, immune biomarkers, and drug sensitivity of the risk-stratified population, aiming to provide new clinical treatment options (Fig. 1).

Materials and methods

RNA-sequencing transcriptomic data collection. RNA-sequencing transcriptomic data and corresponding clinical information were obtained from The Cancer Genome Atlas (TCGA; https://portal.gdc.cancer.gov/). These data included 414 BLCA tissues and 19 normal adjacent tissues. Clinical information, including age, sex, and TNM stage was collected. In total, 29 m7G-related regulatory genes were identified by screening the Gene Set Enrichment Analysis database (GSEA; https://www.gsea-msigdb.org/gsea/index.jsp) and by performing literature searches (18-23). In the BLCA cohort from TCGA, the expression data of these 29 m7G-related genes were extracted for subsequent analysis. The GSE48075 dataset from the Gene Expression Omnibus (GEO) database (http://www.ncbi.nlm.nih.gov/geo) was used as the validation set, and this dataset contained 142 BLCA samples with corresponding survival information and gene expression data.

Identification of m7G regulatory genes in BLCA. Differentially expressed genes (DEGs) involved in m7G methylation were screened between BLCA and normal adjacent tissues using the Wilcoxon test in R (version 4.1.2) (24). Significant results were those with a false discovery rate (FDR) <0.05 and an absolute $\log_2$-fold change >1. Violin plots were drawn using the R package 'vioplot' (version 0.3.7, https://github.com/TomKellyGenetics/vioplot) to show the differential expression of DEGs in BLCA and normal adjacent tissue samples. Spearman correlation analysis was performed to determine associations among DEGs. A protein-protein interaction (PPI) network was obtained through the STRING database (https://string-db.org/) (25) to query the interaction of DEG-related proteins. The Gene Expression Profiling Interactive Analysis (GEPIA) 2 database (http://gepia2.cancer-pku.cn) (26) was also used to validate DEGs in BLCA.

Identification of two clusters with different clinical outcomes based on m7G gene consensus clustering and functional enrichment analysis. Based on DEGs, the BLCA cohort was divided into two distinct subgroups using the R package 'ConsensusClusterPlus' (version 1.36.0, https://rdocumentation.org/packages/ConsensusClusterPlus/versions/1.36.0). Survival curves were drawn to compare the overall survival (OS) between two groups based on Kaplan-Meier analysis. Differences in clinical data (survival status, stage, pathological grade, sex, and age) between the two groups were detected using a χ^2 test. Gene Ontology (GO) and Kyoto Encyclopedia of Genes and Genomes (KEGG) analyses were performed to functionally annotate DEGs in the two subgroups.

Evaluation of the prognostic value of m7G-related regulatory genes in patients with BLCA. Univariate Cox regression analysis was used to estimate the correlation between m7G-related genes and OS. Based on the R package 'glmnet' (version 4.1.3, https://rdocumentation.org/packages/glmnet), the least absolute shrinkage and selection operator (LASSO) Cox regression model was then utilized to narrow down the candidate genes and to develop the prognostic model. Ultimately, the four genes and their coefficients were retained, and the penalty parameter (λ) was decided by the minimum criteria. The gene expression acquired from the LASSO Cox regression and its coefficients were multiplied to generate the risk score to divide patients with BLCA into low- and high-risk groups, and the OS time was compared between the two subgroups via Kaplan-Meier analysis. The 'survival' (version 3.3.0, https://rdocumentation.org/packages/survival), 'survminer' (version 0.4.9, https://CRAN.R-project.org/package=survminer), and 'timeROC' (version 0.4, https://rdocumentation.org/packages/timeROC/versions/0.4) R packages were used to perform receiver operating characteristic (ROC) curve analysis. Differences in clinically relevant variables between different risk groups were evaluated using a χ^2 test and visualized with heatmaps. Moreover, univariate and multivariate Cox regression analyses were performed by using the R packages 'survivalROC' (version 1.0.3, https://rdocumentation.org/packages/survivalROC) and 'survival' to assess whether the risk score was an independent predictor.

Validation of the m7G-related gene prognostic model. To validate the prognostic value of these four m7G-regulated genes, the GSE48075 cohort was used as a validation set. The

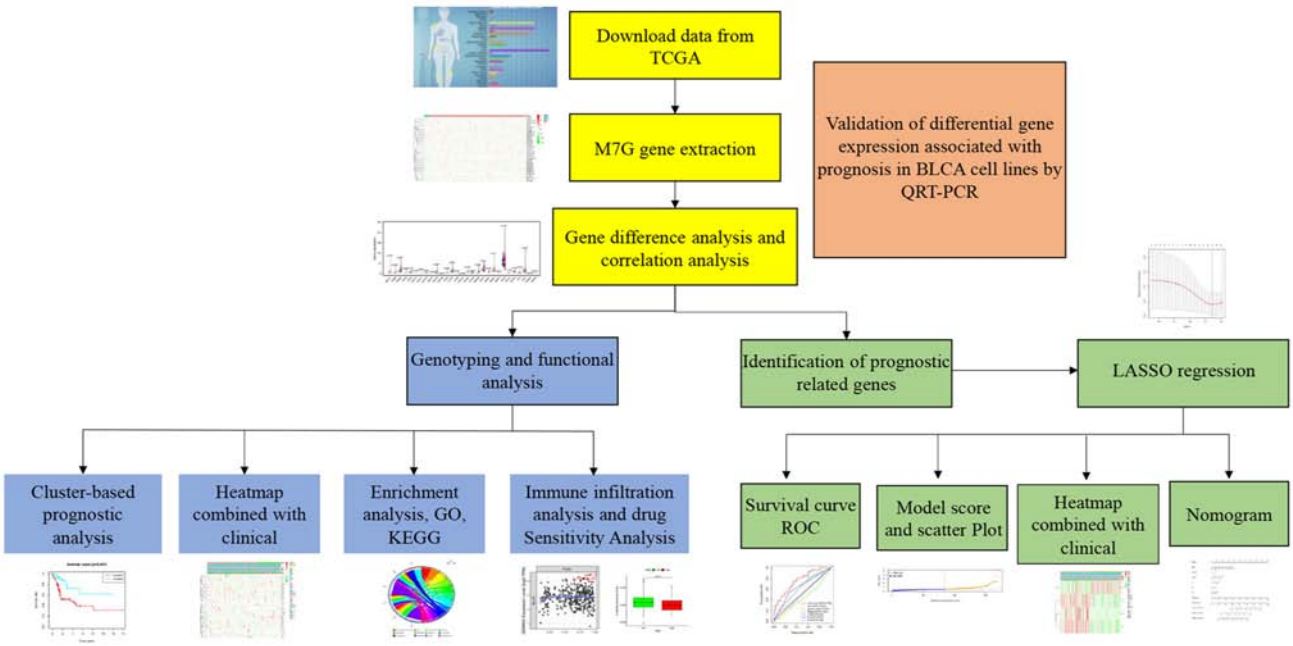

Figure 1. Flowchart of the study. TCGA, The Cancer Genome Atlas; RT-qPCR, reverse transcription-quantitative PCR; GO, Gene Ontology; ROC, receiver operating characteristic; m7G, N7-methylguanosine; BLCA, bladder urothelial carcinoma.

same risk score calculation formula and the same cutoff value that could distinguish between high and low-risk groups were used to classify patients in three cohorts, and Kaplan-Meier survival and ROC curve analyses were performed to evaluate the predictive performance.

Construction of prediction nomogram and decision curve. Based on the R package 'rms' (version 6.2.0, https://rdocumentation.org/packages/rms), clinically relevant factors (histological grade, sex, stage, and age) and risk scores were used to construct prognostic nomograms to predict OS in patients with BLCA. Moreover, the R package 'ggDCA' (version 1.1, https://rdocumentation.org/packages/ggDCA/versions/1.1) was used to finish the decision curve analysis, which could assess whether the present prognostic model could benefit clinical patients.

Tumor immune infiltration analysis. To evaluate the immune function of the aforementioned four m7G-regulated genes, the ImmuCellAI database (http://bioinfo.life.hust.edu.cn) was first utilized to analyze the infiltration of immune cells in BLCA and adjacent tissues. Next, Tumor IMmune Estimation Resource (TIMER; https://cistrome.shinyapps.io/timer) was used to assess the expression of four m7G-related genes with prognostic significance in association with the infiltration of six different immune cell types (B cells, $CD4^+$ T cells, $CD8^+$ T cells, neutrophils, macrophages, and dendritic cells). TIMER is a database that uses high-throughput sequencing data to analyze the infiltration of immune cells in tumor tissues, and mainly provides the infiltration of the above six immune cell types (27). In addition, the TIMER, CIBERSORT, QUANTISEQ, MCPcounter, XCELL, and EPIC algorithms were used to assess immune component profiles, and the R package 'limma' was used for visualization. Furthermore, single sample (ss)GSEA was used to quantify the infiltration and immune function of immune cell subsets with the GSVA R software package (version 1.20.0, https://rdocumentation.org/packages/GSVA/versions/1.20.0). Finally, according to the four-gene expression, boxplots were used to reveal the differential expression of 24 immune checkpoints in the two subgroups of risk stratification, including T cell immune receptor with Ig and ITIM domains (TIGIT), programmed cell death 1 (PD-1), programmed cell death ligand 1 (PD-L1), tumor necrosis factor receptor superfamily, and cytotoxic T lymphocyte-associated protein 4 (CTLA4).

Potential drug prediction. To explore potential compounds associated with four-gene therapy, the four-gene list was input into a connectivity map (Cmap; https://clue.io/), which included gene expression signatures derived from 9 cancer cell lines treated with 2,429 well-annotated compounds. Data from the Cmap were compared with the four-gene signatures to assign connectivity scores. The scores were inversely correlated with the compound's therapeutic effect. Next, IC_{50} values were predicted for standard chemotherapeutics in the low- and high-risk groups with the R package 'pRRophetic' (28).

Validation of the expression of four prognosis-relevant proteins. Immunohistochemistry data from the Human Protein Atlas (HPA; https://www.proteinatlas.org/) was used to validate the protein expression of the four aforementioned prognosis-relevant genes between BLCA and normal bladder tissues from TCGA.

Cell culture and small interfering RNA transfection. Human bladder epithelial cells SV-HUC-1 (cat. no. CRL-9520™), human bladder carcinoma cells 5637 (cat. no. HTB-9™), and T24 (cat. no. HTB-4™) were obtained from ATCC. SV-HUC-1 cells were cultured in Ham's F-12K medium (cat. no. PM150910; Procell Life Science & Technology Co., Ltd.), while 5637 and T24 cells were cultured in RPMI

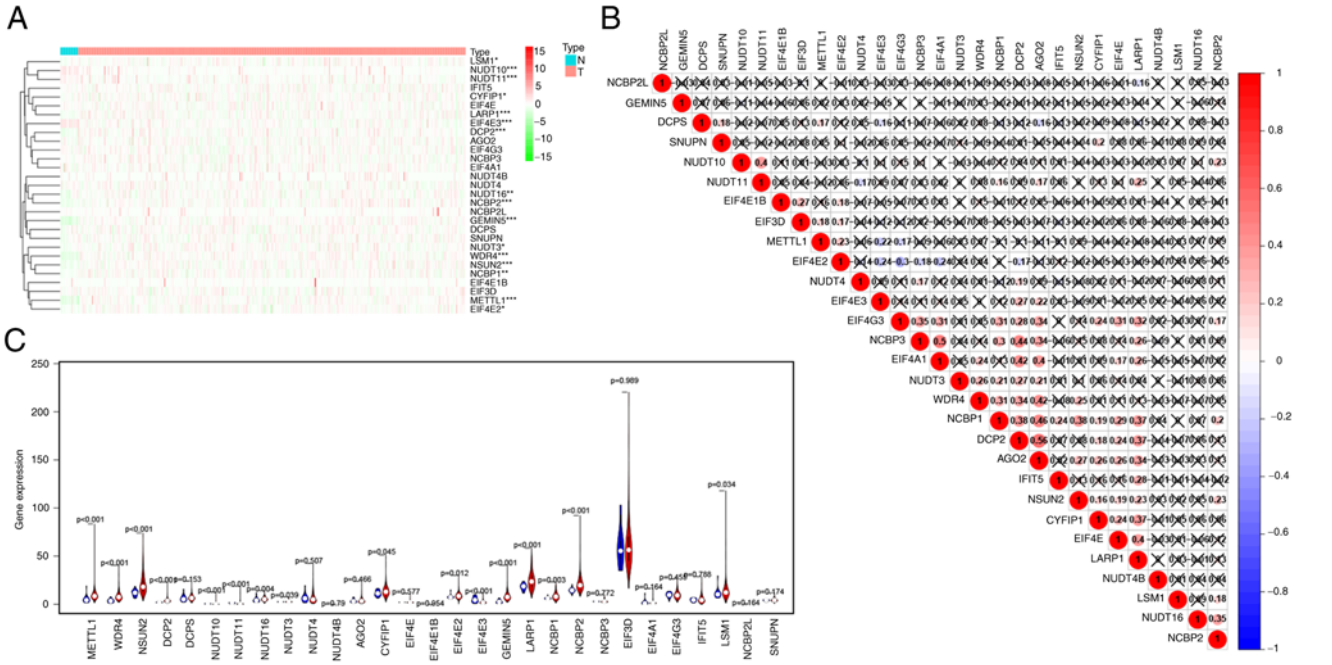

Figure 2. Expression of m7G-modified regulators in BLCA. (A) Heatmap visualization of the expression levels of m7G RNA modification regulators in each sample. Green indicates low expression, whereas red indicates high expression. (B) Spearman's correlation analysis of the 29 m7G RNA modification regulators in BLCA. *P<0.05, **P<0.01, ***P<0.001. (C) Violin plot displaying m7G RNA modification regulators in BLCA. Blue represents normal samples and red represents BLCA samples. The white dot represents the median value of expression. m7G, N7-methylguanosine; BLCA, bladder urothelial carcinoma; N, normal samples; T, tumor samples.

1640 medium (cat. no. C11875500BT; Gibco; Thermo Fisher Scientific, Inc.). All media were supplemented with 10% heat-inactivated FBS (cat. no. B-9™) and T2 and 1% penicillin-streptomycin (cat. no. 15070063; Gibco; Thermo Fisher Scientific, Inc.). The cells were kept in a 37˚C incubator with 5% CO_2. Small interfering (si) gem nuclear organelle-associated protein 5 (GEMIN5) was designed and synthesized by Guangzhou RiboBio Co., Ltd. and transfected with Lipofectamine® 3000 (Thermo Fisher Scientific, Inc.). At 48 h post-transfection, the cells were collected for functional experiments. The interference efficiency was detected by reverse transcription-quantitative PCR (RT-qPCR).

RT-qPCR. Total RNA was extracted from the three cell types using TRIzol® reagent (cat. no. 15596-026; Ambion; Thermo Fisher Scientific, Inc.). cDNA was synthesized using a cDNA reverse transcription kit (cat. no. EP0751; Thermo Fisher Scientific, Inc.). cDNA was used as a template, and the β-actin gene was used as the internal reference for normalizing the RT-qPCR data. A two-step standard PCR amplification procedure was conducted according to the manufacturer's instructions (cat. no. 10222ES60; Shanghai Yeasen Biotechnology Co., Ltd.). The relative expression of the target gene was calculated using the $2^{-\Delta\Delta Cq}$ method (29). The primers used are shown in Table SI.

Cell viability and colony formation assays. The viability of T24 and 5637 cells was detected using a Cell Counting Kit-8 (CCK-8) assay kit (cat. no. BS350B; Beijing Labgic Technology Co., Ltd.) according to the manufacturer's instructions. The optical density was measured with a microplate reader (Thermo Fisher Scientific, Inc.) at a wavelength of 450 nm. The cell viability values of each group were detected after 24, 48, and 72 h. For the colony formation assays, cells in the logarithmic growth stage were collected, and 1,000 cells were plated in six-well plates. The cells were cultured for 10 days, fixed with methanol at room temperature for 20 min, and stained with 0.1% crystal violet at room temperature for 15 min. The colonies were imaged and counted using light microscopy. The number of colonies consisting of ≥50 cells was counted.

Statistical analysis. All data were statistically analyzed using R. FDR was used in GO and KEGG analyses. Gene expression and immune infiltration levels were calculated using a paired Student's t-test or Wilcoxon test. Differences in OS between groups were compared using Kaplan-Meier analysis. Independent predictors were evaluated using Cox regression analysis. A two-tailed P<0.05 was considered to indicate a statistically significant difference.

Results

Identification of differentially expressed m7G-related genes in BLCA. Differential expression analysis of 29 m7G-regulated genes was performed in BLCA (n=414) and adjacent normal tissues (n=19). The heatmap showed that 17 of these m7G modification regulators were differentially expressed between BLCA and normal tissues (Fig. 2A). The expression levels of METTL1, WDR4, NSUN2, DCP2, nudix hydrolase (NUDT)10, NUDT11, NUDT16, NUDT3, AGO2, cytoplasmic FMR1 interacting protein 1 (CYFIP1), EIF4E2, EIF4E3, GEMIN5, LARP1, NCBP1, NCBP2, and LSM1 were higher in BLCA tissues than in normal tissues (Fig. 2B). Fig. 2C showed that

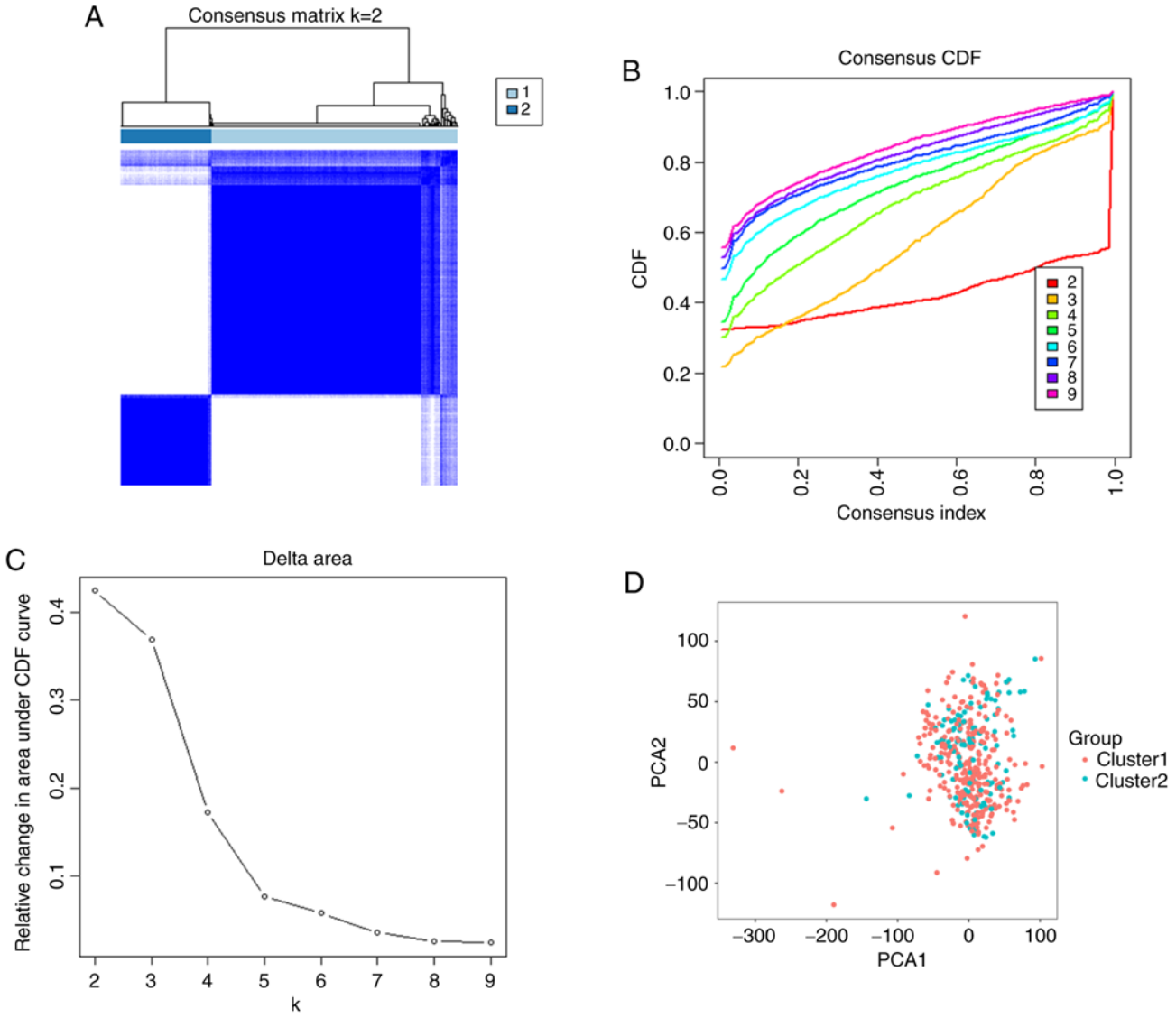

Figure 3. Consistent cluster analysis of data of patients with bladder cancer. (A) Correlation between subgroups when the number of clusters is k=2. (B) The CDF is shown when k=2-9. (C) Relative change in the area under the CDF curve when k=2-9. (D) Principal component analysis of RNA-sequencing data. The red dots represent cluster 1, while the cyan dots represent cluster 2. CDF, cumulative distribution function.

the correlation between GEMIN5 and LARP1 was the most significant (correlation coefficient, 0.71). The GEPIA2 database results showed that the expression of EIF4E3, NUDT10, NUDT11 and METTL1 significantly differed between the two groups (Fig. S1). RT-qPCR was performed to confirm the expression of prognostic m7G-related genes in bladder cancer cells. A total of 17 gene symbols were imported into the STRING database to generate the PPI network. The genes with the highest clustering coefficient were LARP1, GEMIN5, NUDT11, NUDT10, and WDR4 (Fig. S2).

Identification of two clusters of patients with BLCA with distinct clinical outcomes using consensus clustering based on m7G RNA-modification regulators. To further explore the clinical relevance of m7G RNA-modifying modulators, patients with BLCA were clustered into subgroups according to the differential gene expression. Based on the similarity of m7G-related genes, k=2 produced the best clustering, and patients with BLCA could be divided into two distinct and non-overlapping groups (Fig. 3A-C). Principal component analysis was used to validate the results of clustering (Fig. 3D). Subsequently, whether there were significant differences in OS, stage, age, grade, or sex between these two clusters was evaluated. The results showed that the prognosis in cluster 2 was significantly better (P<0.01) than that of cluster 1 (Fig. 4B), but no significant differences were observed in age, sex, histological grade, or pathological stage between the two clusters (Fig. 4A). Next, the m7G genes associated with prognosis were screened out for in-depth analysis based on a heat map. The results of consensus clustering showed a strong association between the expression patterns of m7G-related genes and clinical parameters.

Functional enrichment analysis of m7G RNA-modification regulators. GO and KEGG enrichment analyses were performed on the DEGs between clusters 1 and 2 to investigate the results of clustering from the perspective of associated pathways and biological processes. According to

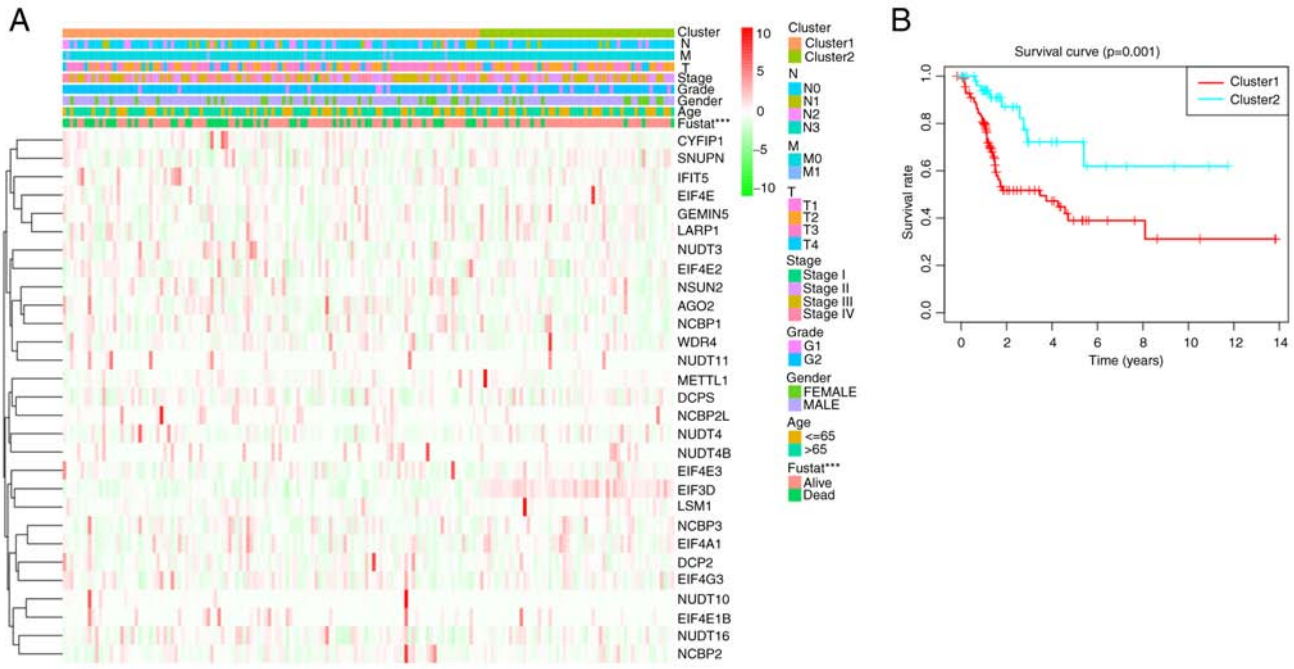

Figure 4. Differences in the clinicopathological characteristics and OS for the two clusters. (A) Heatmap and clinicopathological features of the two clusters. Green indicates low expression, while red indicates high expression. (B) Comparison of OS between groups 1 and 2. ***P<0.001. OS, overall survival.

the results of the GO enrichment analysis, the upregulated genes were primarily enriched in 'Extracellular matrix organization', 'Extracellular structure organization', 'External encapsulating structure organization', 'Phagocytosis, recognition', 'Complement activation, Classical pathway', 'Humoral immune response mediated by circulating immunoglobulin', 'Phagocytosis, engulfment', 'Complement activation', and 'B cell receptor signaling pathway' (Fig. 5A and B). KEGG enrichment analysis results showed that these upregulated genes were significantly enriched in 'Proteoglycans in cancer', 'Wnt signaling pathway', 'ECM-receptor interaction', and 'PI3K-Akt signaling pathway' (Fig. 5C and D).

Construction of a prognostic model based on four m7G-regulated genes. Based on the association between m7G RNA methylation regulators and the OS of patients with BLCA, Univariate Cox regression analysis was performed on the expression levels of the 29 important regulators to explore the clinical relevance. The results showed that 9 of the 29 genes were notably associated with OS (P<0.05). As shown in Fig. 6A, NUDT10, NUDT11, AGO2, CYFIP1, GEMIN5, LARP1, and NCBP1 were considered risk genes with a hazard ratio (HR) >1, whereas NUDT4 and eukaryotic translation initiation factor 3 subunit D (EIF3D) were considered protective genes with HR<1.

LASSO Cox regression analysis identified 9 genes with the strongest predictive ability (Fig. 6B and C). Based on the corresponding coefficients in the LASSO algorithm, four optimal genes (NUDT11, CYFIP1, GEMIN5, and EIF3D) were selected to establish the BLCA risk model (Fig. 6D). The risk score was calculated as follows: Risk score=(0.289x expression value of NUDT11) + (0.503x expression value of CYFIP1) + (0.979x expression value of GEMIN5)-(0.807x expression value of EIF3D).

To explore the prognostic role of these four-gene signature models, patients with BLCA were divided into low- and high-risk groups according to the median risk score. The risk score distribution of patients with BLCA was plotted (Fig. 7A), and the survival status of patients with BLCA was evaluated using a dot matrix (Fig. 7B). Survival analysis showed that patients with high-risk scores had a poorer OS than those with low-risk scores (Fig. 8A; P<0.001). The 5-year OS rate was 67.3% in the low-risk group and 24.5% in the high-risk group. The ROC curve analysis results showed that the area under the curve (AUC) at 1-, 3- and 5-year OS was 0.755, 0.745, and 0.758, respectively, thus showing good predictive power for survival outcome (Fig. 8B). A heatmap with clinical relevance showed the differential expression of the four prognostic genes in the high- and low-risk groups (Fig. 9A). Of note, significant differences in clinical parameters such as fustat (P<0.001), stage (P<0.01) and grade (P<0.05) were observed.

GEO database validates the predictive performance of the risk model. To estimate the predictive capability of four-gene signatures in GEO datasets, the GSE48075 dataset was used for validation. A total of 57 patients with BLCA in the GSE48075 cohort were divided into low- (n=29) and high-risk (n=28) groups according to the cutoff value of TCGA cohort. The results of survival analysis showed that patients with BLCA in the low-risk group had a significantly better OS compared with that of patients in the high-risk group (P=0.014; Fig. 8C), which was consistent with the results on the training set. The AUCs for 3-year OS was 0.685, suggesting that the risk model had a good predictive ability in BLCA (Fig. 8D). Since this cohort did not survive >5 years, no 5-year ROC curves were drawn.

Four-gene risk signature independently predicts prognosis in patients with BLCA. Upon removing samples without

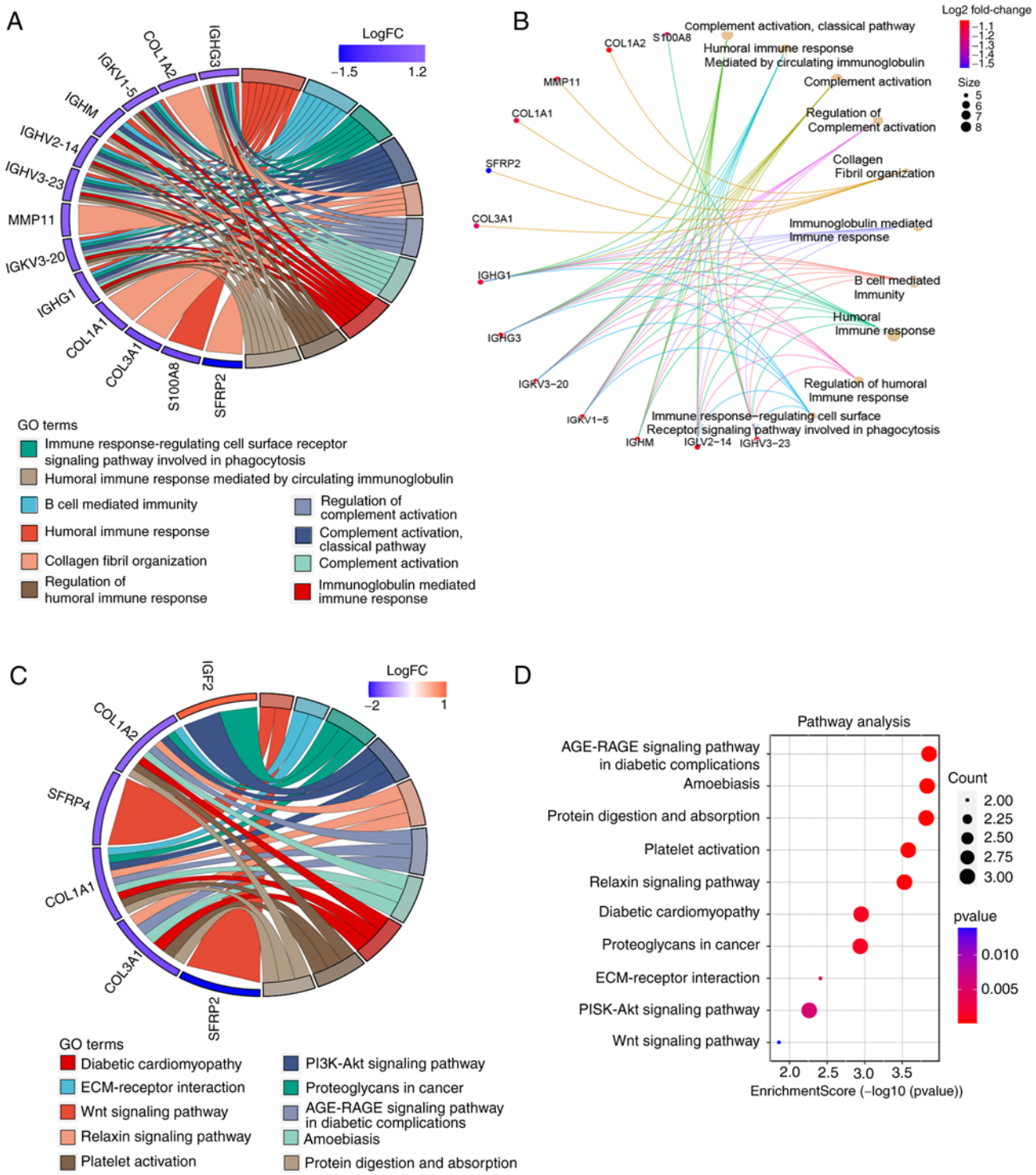

Figure 5. GO and KEGG analyses of differentially expressed genes between two clusters. Functional annotation of highly expressed genes in cluster 1 using (A and B) GO terms and (C and D) KEGG pathway. GO, Gene Ontology; KEGG, Kyoto Encyclopedia of Genes and Genomes.

complete clinical information, 170 samples were qualified for Cox regression analysis. Cox univariate analysis indicated that stage and the four-gene risk score were significantly associated with OS in patients with BLCA (P<0.001; Fig. 9B). Multivariate Cox regression analysis was performed to assess whether risk score was independent of other clinicopathological features as a predictor for BLCA, and the results showed that the risk score of patients with BLCA was independently associated with OS (P<0.001; Fig. 9C). In conclusion, these results indicated that the four-gene risk signature could be used to predict the prognosis of patients with BLCA independently of other clinicopathological features such as sex, histological grade, age, or pathological stage.

Construction of a nomogram. To facilitate the clinical application of four-gene risk signature, a detailed prognostic nomogram based on histological grade, sex, pathological stage, age, and risk score was established (Fig. 10A). The nomogram

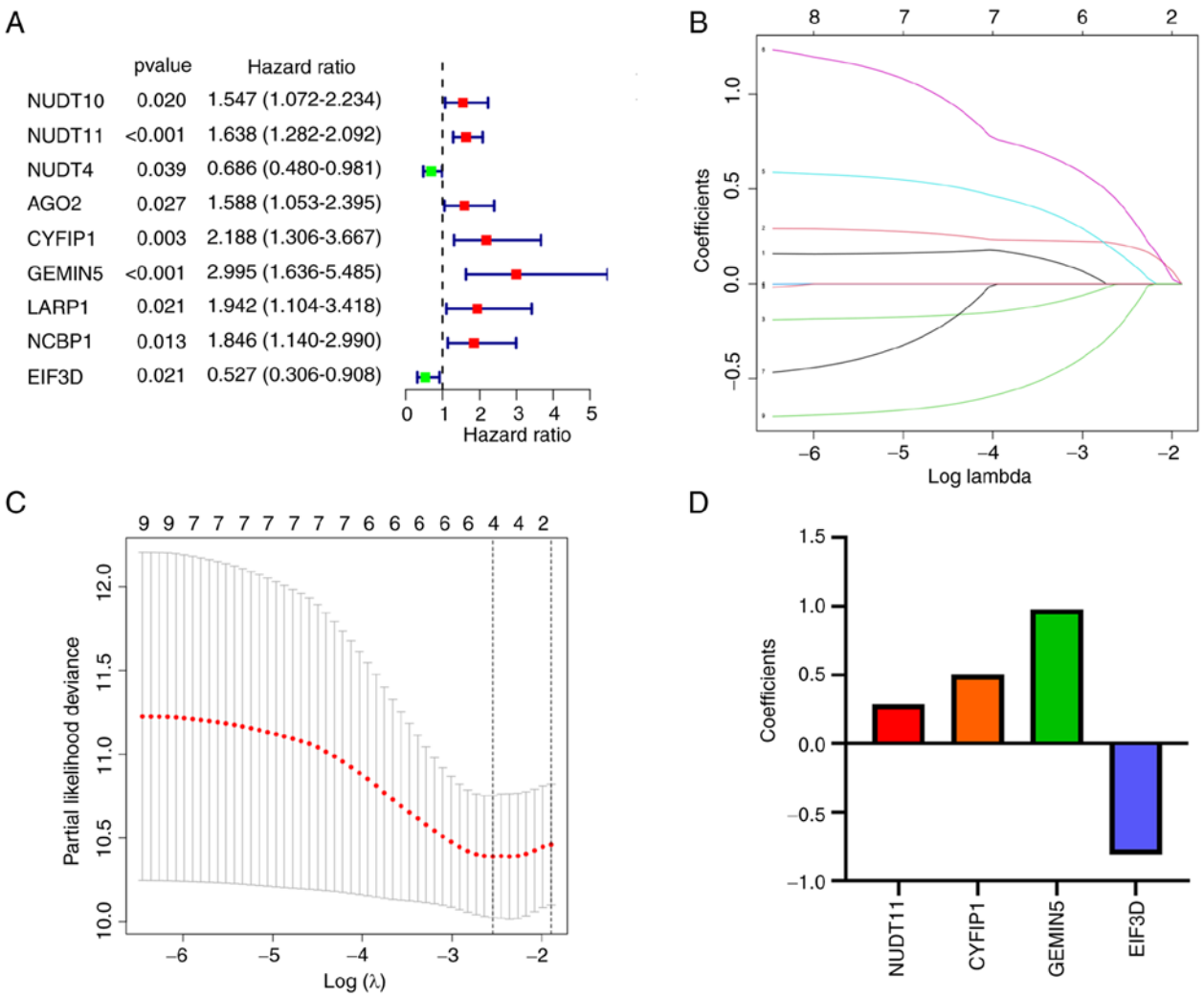

Figure 6. Establishment of a prognostic risk model based on m7G RNA modification-regulated genes. (A) Univariate Cox regression analysis of m7G RNA methylation regulators. (B-D) Construction of the gene signature using least absolute shrinkage and selection operator Cox regression. m7G, N7-methylguanosine.

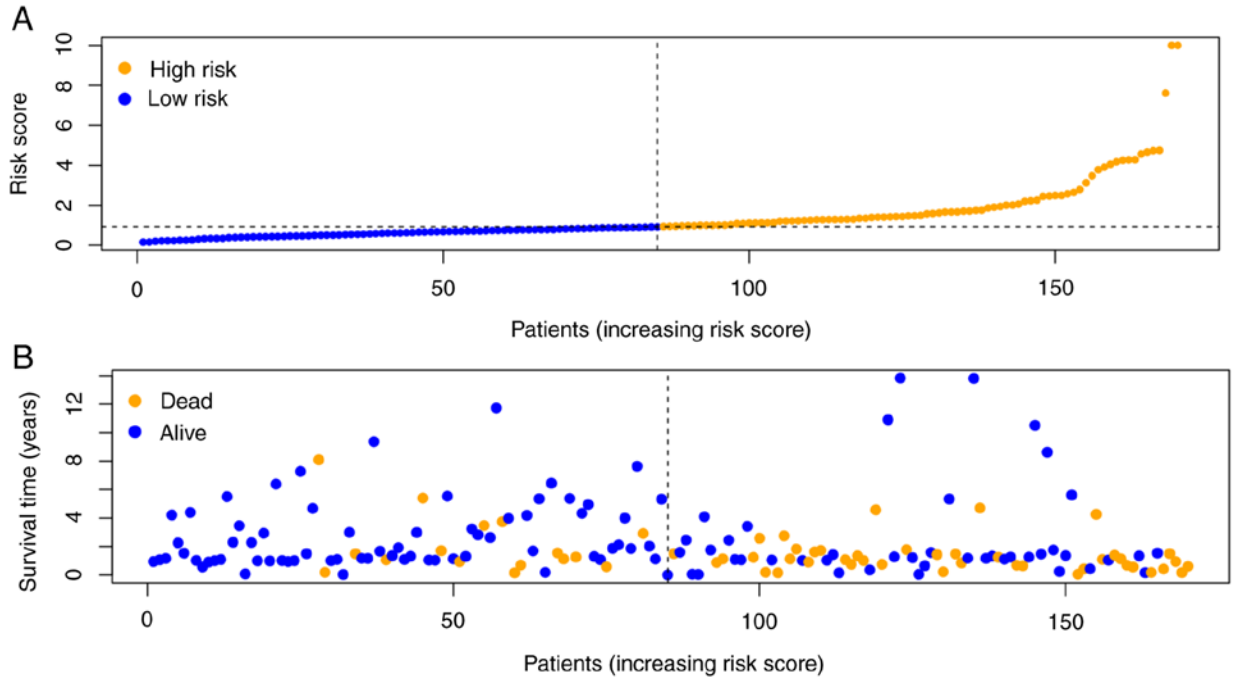

Figure 7. Evaluation of prognostic models. Distribution of (A) risk scores and (B) survival status in the prognostic model.

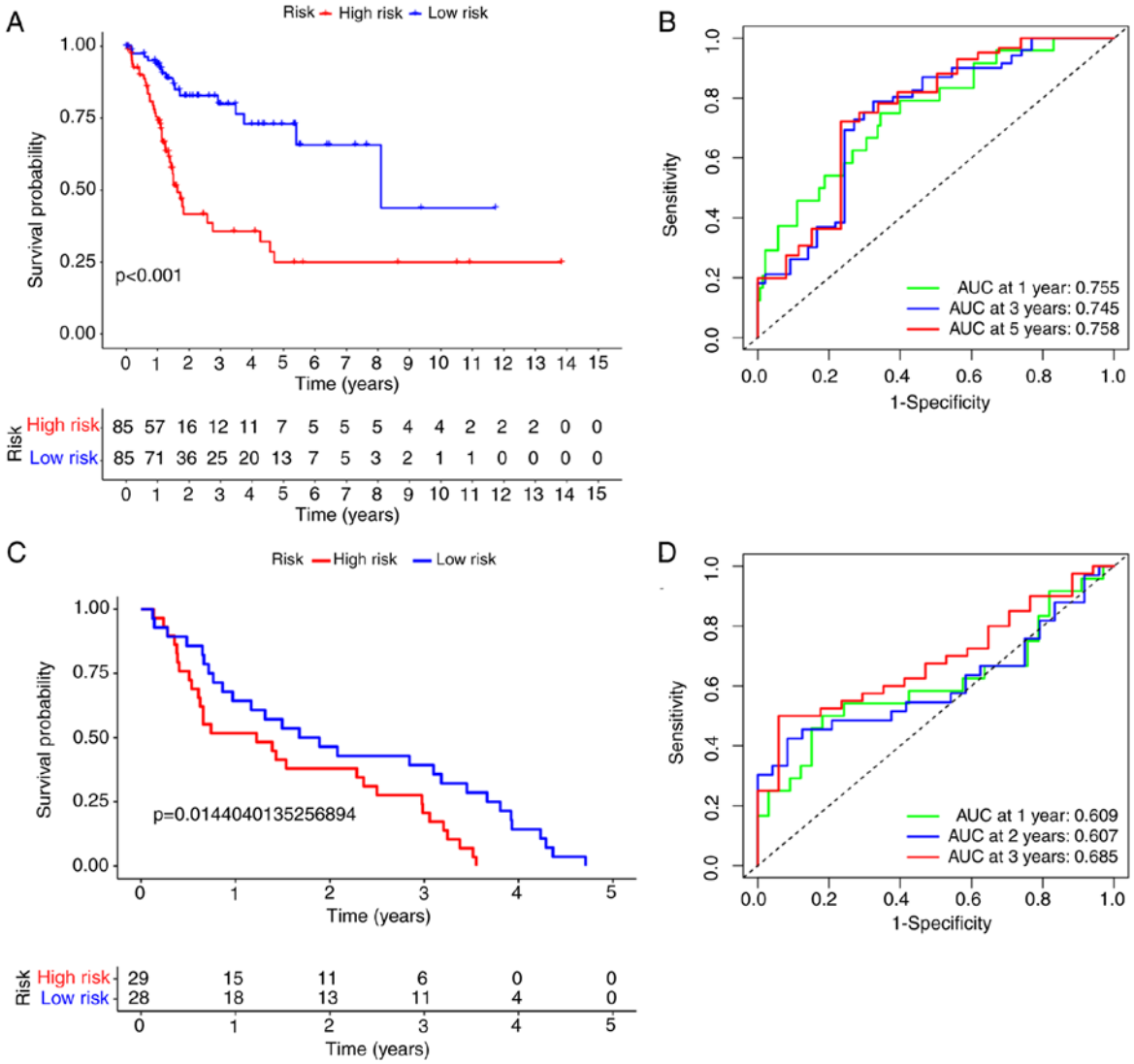

Figure 8. Kaplan-Meier survival analysis of the prognostic model. Patients in both datasets were assigned to low-risk (blue) or high-risk (red) groups, using the median risk score as the cutoff value. (A) Survival curve analysis of TCGA cohort. In TCGA cohort, the low-risk group had a higher probability of survival than that of the high-risk group (P<0.001). (B) ROC curve analysis of TCGA cohort. The 1-, 3-, and 5-year AUCs were 0.755, 0.745, and 0.758, respectively. (C) Survival curve analysis of the GEO cohort. The low-risk group had a higher probability of survival than that of the high-risk group (P=0.014). (D) ROC curve analysis of the GEO cohort. The 1-, 2-, and 3-year AUCs were 0.609, 0.607, and 0.685, respectively. TCGA, The Cancer Genome Atlas; ROC, receiver operating characteristic; AUC, area under the curve; GEO, Gene Expression Omnibus.

could precisely predict 1-, 3-, and 5-year OS in patients with BLCA. The AUC for risk score was 0.76, which indicated that this model had good predictive value for patients with BLCA (Fig. 10B). Nomogram-based clinical decisions had a higher net benefit compared with that of individual predictors (Fig. 10C).

Correlation of prognosis-related m7G genes with immune infiltration. GO and KEGG enrichment analyses indicated that m7G-related gene functions primarily involve the activation of cancer-related signaling pathways, affecting complement and B cell activity. Further immune infiltration analysis revealed significant differences in normal adjacent and BLCA tissues. Differential expression of immune cells (Fig. 11A-Q) indicated that tumor immune infiltration is important in patients with BLCA. According to the TIMER, CIBERSORT, QUANTISEQ, and MCPCOUNTER algorithms, the expression levels of $CD8^+$ T cells, $CD4^+$ T cells, neutrophils, macrophages, and monocytes in the high-risk group were higher than those in the low-risk group (Fig. 11R), suggesting that immune infiltration may influence patient outcomes. Quantifying enrichment fractions implied that the prognosis in the high-risk groups may be affected by antigen-presenting cells' function, chemokine receptor, immune checkpoint expression, and parainflammation (Fig. 11S).

The TIMER database was used to investigate the link between the expression levels of four genes and immune infiltration. After adjusting for purity, the expression of GEMIN5 (Fig. 12A) was positively correlated with $CD8^+$ T cells ($P=1.27\times10^{-9}$), dendritic cells ($P=7.63\times10^{-8}$), and neutrophils ($P=3.48\times10^{-6}$). NUDT11 expression levels were correlated with the number of $CD8^+$ T cells ($P=8.47\times10^{-4}$), $CD4^+$ T cells ($P=3.03\times10^{-2}$), dendritic cells ($P=1.36\times10^{-3}$), macrophages ($P=1.78\times10^{-5}$) and neutrophils ($P=6.92\times10^{-3}$) (Fig. 12B). EIF3D expression levels were negatively correlated with macrophage levels ($P=1.78\times10^{-5}$) (Fig. 12C). CYFIP1

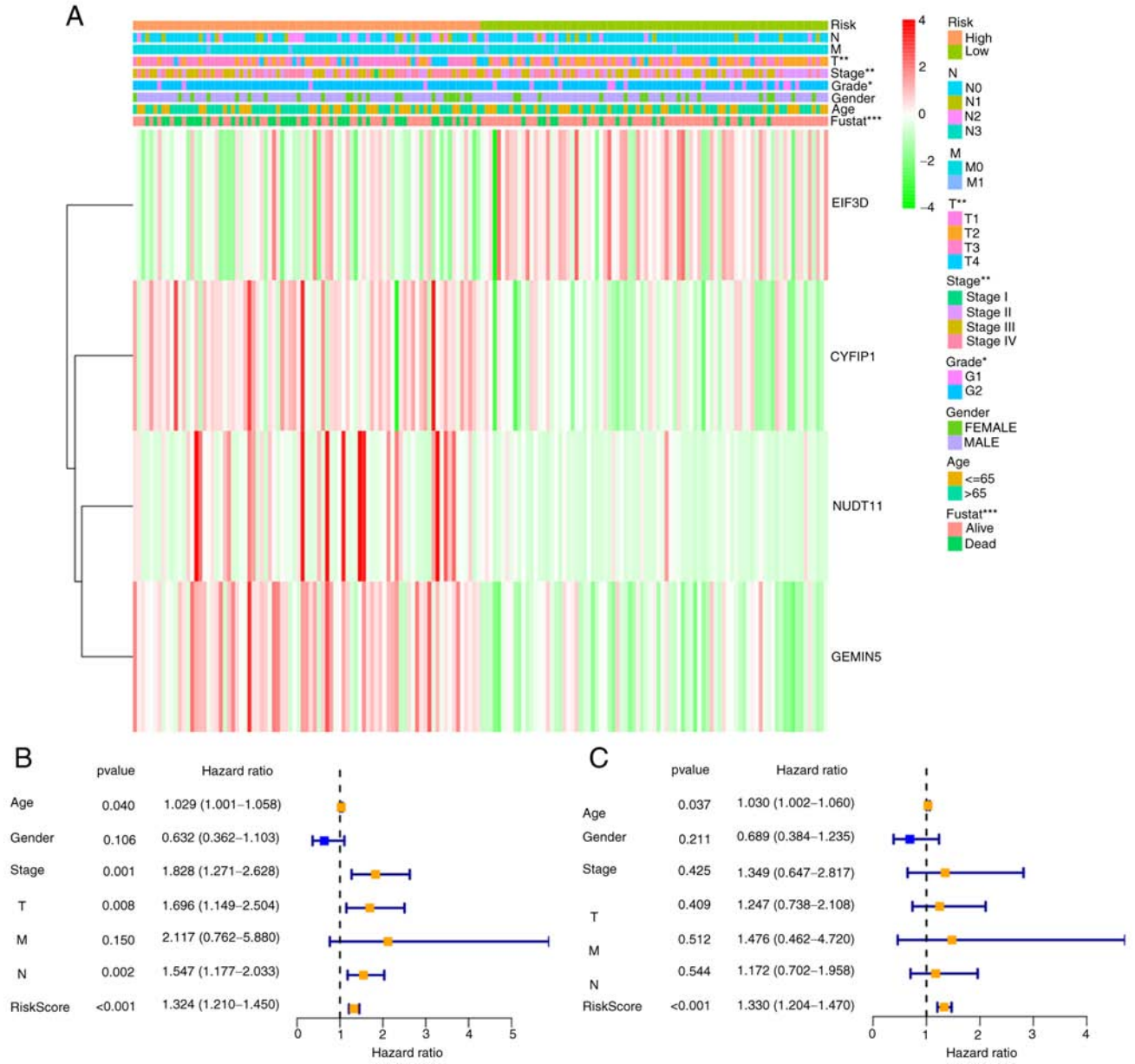

Figure 9. Impact of risk scores and clinicopathological features on prognosis in patients with bladder urothelial carcinoma. (A) Heatmap showing the distribution of clinicopathological features and the expression of four N7-methylguanosine RNA-modifying regulators in high- and low-risk populations. (B) Univariate and (C) multivariate Cox regression analyses of clinicopathological parameters and overall survival. *P<0.05, **P<0.01, ***P<0.001.

expression levels were significantly correlated with the number of B cells (P=3.57x10^{-2}), CD8^{+} T cells (P=1.23x10^{-9}), dendritic cells (P=1.94x10^{-6}), macrophages (P=4.7x10^{-7}) and neutrophils (P=7.4x10^{-8}) (Fig. 12D). As shown in Fig. S3, copy number loss of NUDT11 resulted in reduced B cell and neutrophil infiltration, while loss of GEMIN5 and CYFIP1 copy number reduced the infiltration of CD4^{+} T cells. Loss of EIF3D copy number resulted in increased levels of dendritic cells. Kaplan-Meier curve results indicated that enrichment of the four genes in CD8+ T cells was associated with a poorer prognosis in patients with BLCA.

Exploring a potential treatment for patients with BLCA based on four genes. A clear association was found between high-risk patients stratified based on four genes and the expression of various immune checkpoints, such as CTLA4, PD-1, PD-L1, and PD-L2 (Fig. 13A). Immune checkpoint inhibitors may be effective in these patients. Sensitivity analysis of chemotherapeutic drugs showed that A.443654, A.770041, docetaxel, and pazopanib were effective in low-risk groups, while axitinib, cisplatin, sorafenib, vinblastine, and vinorelbine may be more effective in high-risk groups. There was no difference in the sensitivity to doxorubicin between the two groups (Fig. 13B). All DEGs were divided into up and downregulated groups and uploaded to the CMap database to identify candidate small molecule drugs for treating BLCA. With P<0.01 and n>2 as the screening criteria, 10 small-molecule drugs with treatment effects on BLCA were identified: BRD-K50174388, I-BET-762, beclomethasone-dipropionate, BRD-K64233461, KU-C104131, BRD-K41668190, erlotinib, BRD-K53120552, BRD-K23021002, and heptaminol (Table I). A negative enrichment score represented an inhibitory effect.

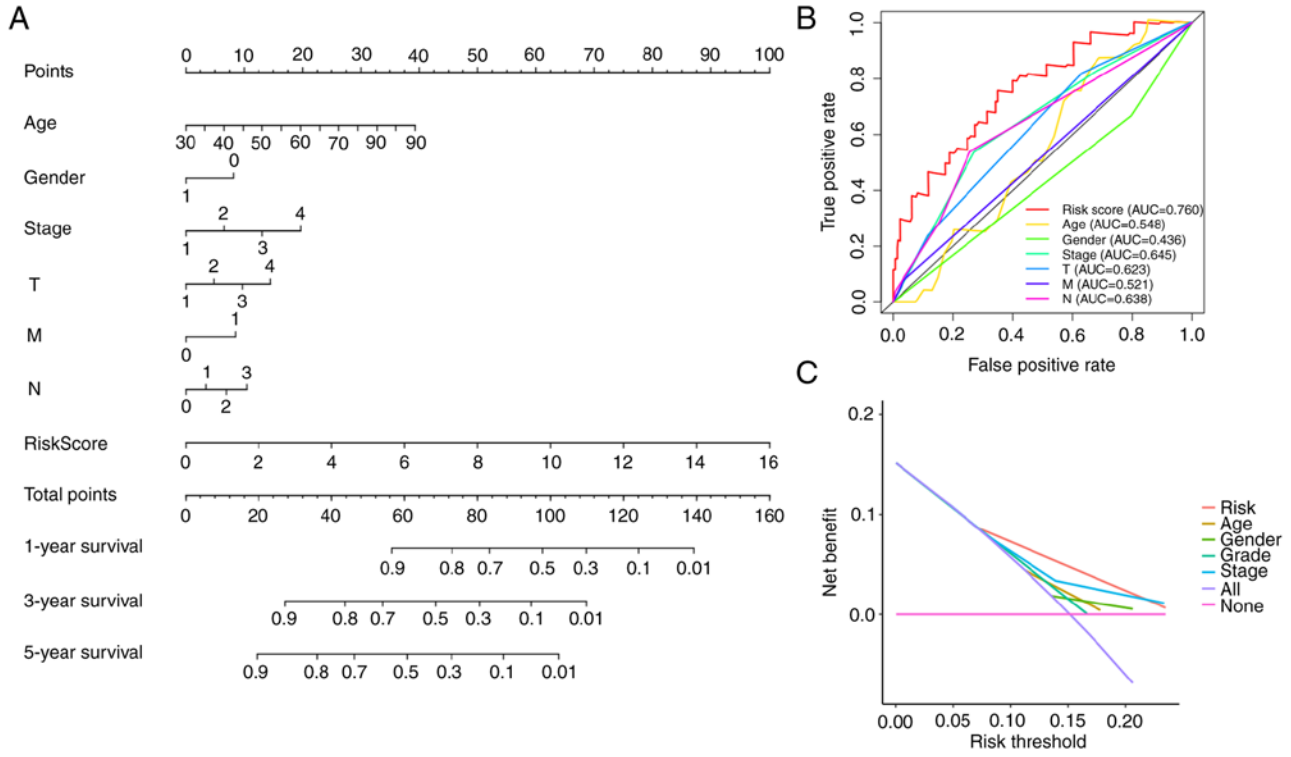

Figure 10. Prognostic nomogram and ROC curve analysis. (A) The 1-, 3-, and 5-year overall survival of patients with BLCA could be systematically predicted by combining clinical data with prognostic nomograms. (B) Evaluation of the predictive performance of the model by ROC curve analysis. (C) Decision curve analysis was used to evaluate the clinical utility of different decision strategies. The red line represents the nomogram. ROC, receiver operating characteristic.

Immunohistochemistry validation based on the HPA database. As shown in Fig. S4, the protein expression levels of GEMIN5 and CYFIP1 were elevated in BLCA compared with those in normal bladder tissues. NUDT11 expression was more evident in normal bladder tissues than in cancer tissues. Of note, EFI3D was not included in the figure as it was not included in the aforementioned database.

RT-qPCR-mediated verification of the mRNA expression of four genes in BLCA cell lines. The RT-qPCR results showed that GEMIN5, CYFIP1, and EIF3D exhibited high levels of expression in T24 and 5637 cells, while NUDT11 exhibited a high expression level in SV-HUC-1 cells. The results were statistically significant (Fig. 14).

Knockdown of GEMIN5 suppresses bladder cancer cell proliferation. To validate the BLCA proliferation-promoting ability of m7G-associated genes, GEMIN5 was selected, since it had the highest HR value in the risk model, to perform CCK-8 and colony formation assays. si-GEMIN5 was used to knock down the expression of GEMIN5 in T24 and 5637 cells, and si-GEMIN5-1 had the best knockdown effect (Fig. 15A). CCK-8 (Fig. 15B) and colony formation (Fig. 15C) assays revealed the that knockdown of GEMIN5 inhibited the proliferation of T24 and 5637 cells.

Discussion

BLCA is a lethal solid tumor with complex molecular and cellular heterogeneity (30). Molecular markers associated with BLCA presently used in the clinic include urinary nuclear matrix protein 22, bladder tumor antigen, and fibrin degradation product. However, these tumor markers have low specificity and poor predictive ability. Thus, there is an urgent need to identify novel BLCA biomarkers that have i) predictive and prognostic value, ii) diagnostic value, and iii) can be used to support the development of personalized treatment plans. With the development of bioinformatics-based techniques, numerous studies have confirmed the predictive role of novel biomarkers in BLCA (31-33).

As a relatively more recently identified mechanism of gene regulation, RNA m7G modification has attracted large interest recently. m7G is a general tRNA modification in prokaryotes and eukaryotes, and is catalyzed by METTL1/WDR4, an integral complex involved in epigenetic regulation (34). m7G at position 46 of tRNA is present in the variable loop, and it is likely that METTL1 reduces tRNA stability by affecting this structure (35). In addition to tRNAs, m7G regulates the translation of mRNA. Different methyltransferases incorporate m7G onto different mRNAs and/or into secondary structure motifs, thus exerting effects on mRNAs, including translation (36). A general mechanism has been found to be involved in m7G-mediated cancer, in which impaired m7G selectively suppresses the translation efficiency of oncogenic mRNAs with a higher frequency of m7G tRNA cognate codons by prolonging ribosome pausing periods (37). As evidence of the regulatory role of m7G in mRNA and microRNA regulation is continuously being uncovered, it is necessary to investigate the role of RNAs other than tRNA.

Although the study of m7G modification in the field of cancer is still in its infancy, combined with bioinformatics analysis, it may still provide clues for subsequent basic and

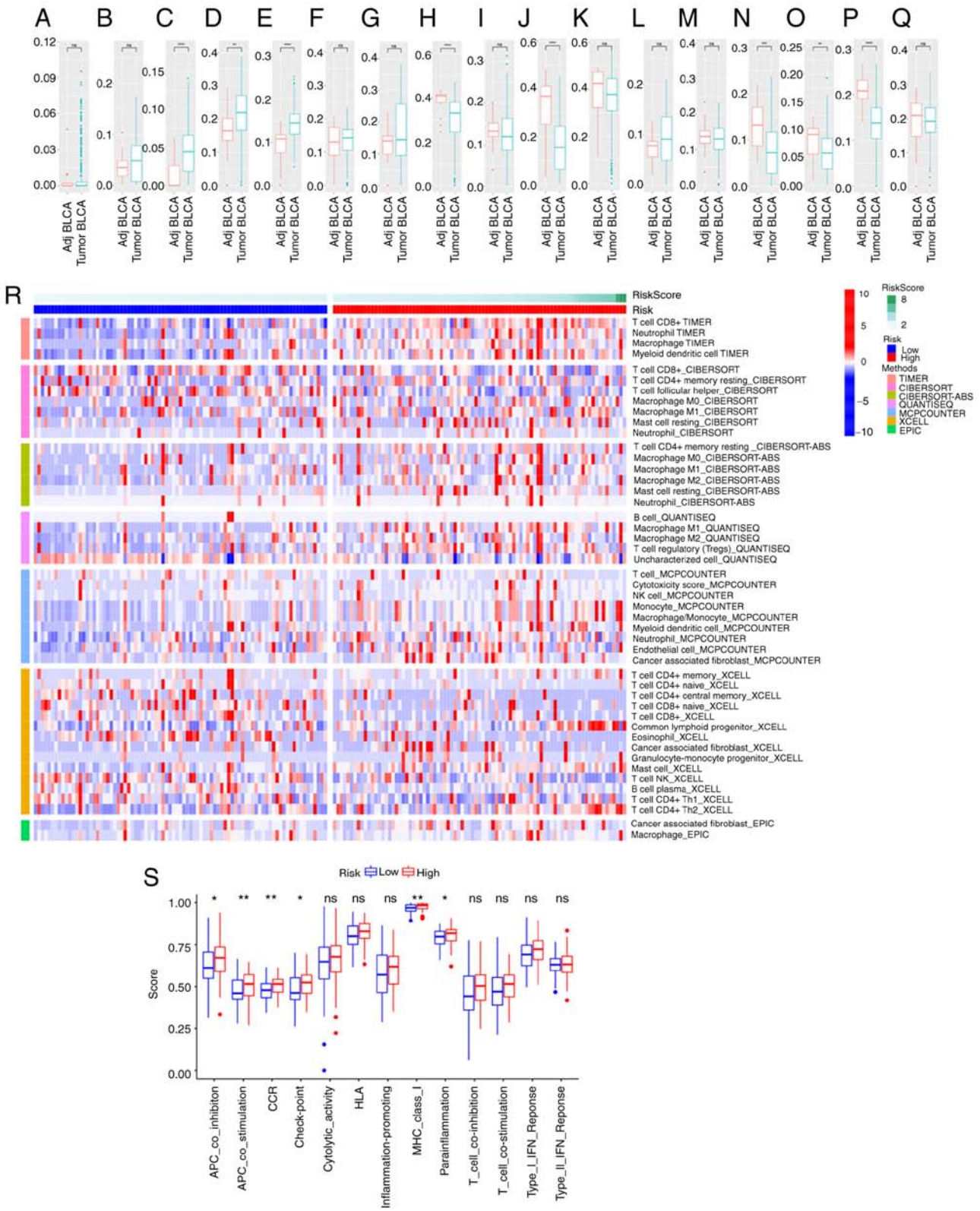

Figure 11. Immune infiltration landscape and functional analysis. Differential expression of immune cells in normal and tumor tissues: (A) CD4 naive T cells; (B) CD8 naive T cells; (C) Effector memory T cells; (D) Induced Tregs; (E) Natural Tregs; (F) Type 1 regulatory cells; (G) Th1 cells; (H) Th2 cells; (I) Th17 cells; (J) T follicular helper cells; (K) Cytotoxic T cells; (L) Exhausted T cells; (M) Mucosal-associated invariant T cells; (N) Natural killer cells; (O) γΔ cells; (P) $CD4^+$ T cells; and (Q) $CD8^+$ T cells. (R) Association between risk score and altered immune landscape. Heatmap for anticancer immunity cycles pattern. (S) Single-sample Gene Set Enrichment Analysis was used to correlate immune cell subsets and related functions. *P<0.05, **P<0.01, ***P<0.001. Tregs, regulatory T cells; Th, helper T cell.

clinical research. The present study demonstrated that the majority of m7G-related genes were expressed at higher levels in BLCA than in non-BLCA tissues, and identified four genes associated with BLCA prognosis (namely GEMIN5, NUDT11,

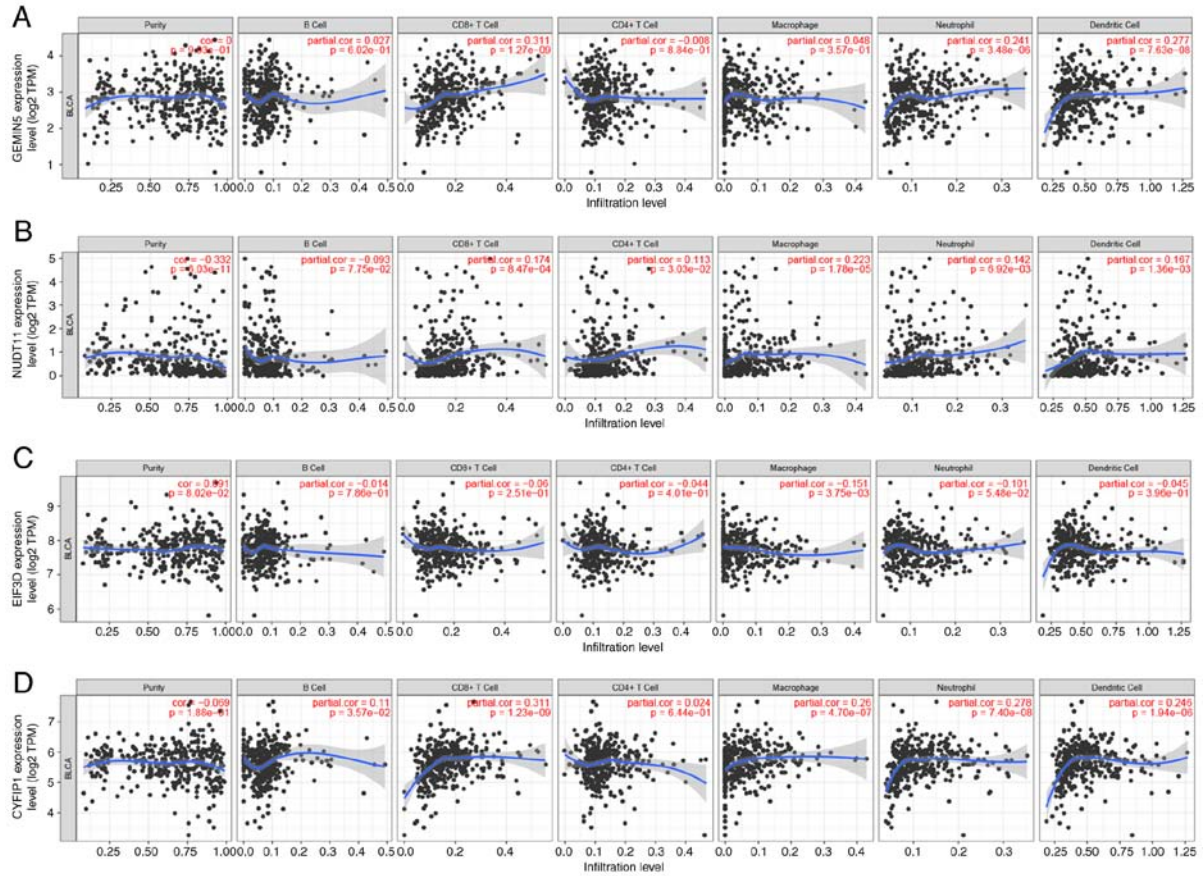

Figure 12. Association between N7-methylguanosine-related gene expression and proportion of immune infiltration. Purity, B cells, CD8$^+$ T cells, CD4$^+$ T cells, macrophages, neutrophils and dendritic cells. (A) Gem nuclear organelle-associated protein 5. (B) Nudix hydrolase 11. (C) Eukaryotic translation initiation factor 3 subunit D. (D) Cytoplasmic FMR1 interacting protein 1. TPM, transcripts per million.

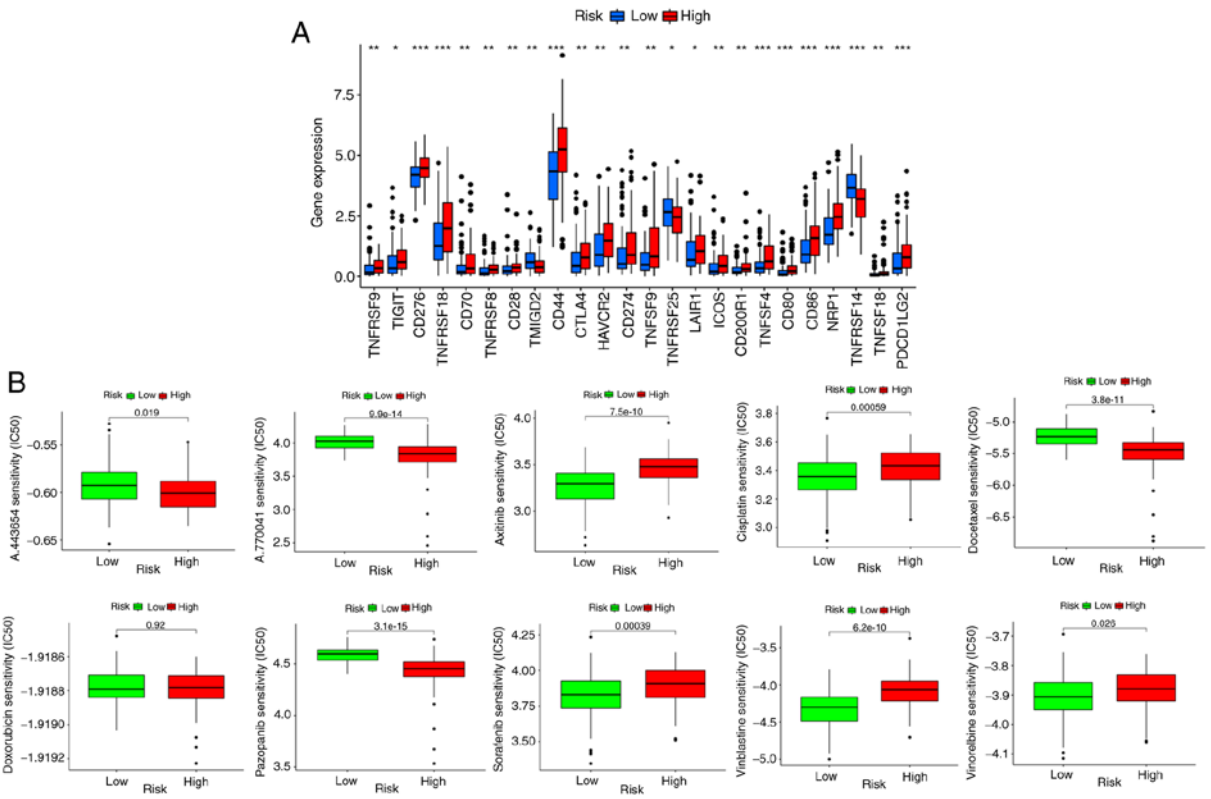

Figure 13. Potential treatment for patients with BLCA based on four genes. (A) Different expression of immune checkpoints in high and low-risk patients. (B) Potential drugs for patients with BLCA. *P<0.05, **P<0.01, ***P<0.001. BLCA, bladder urothelial carcinoma.

Table I. The top 10 small molecule drugs in the connectivity map dataset.

Compounds	Enrichment	P-value	n	Percent non-null (%)	Type
BRD-K50174388	-0.6759	0.0081[a]	3	100	NA
I-BET-762	-0.6758	0.0025[a]	3	100	Bromodomain inhibitor
Beclomethasone-dipropionate	-0.6758	0.0025[a]	3	100	Immunosuppressant
BRD-K64233461	-0.6757	<0.001[b]	3	100	NA
KU-C104131	-0.6757	<0.001[b]	3	100	NA
BRD-K41668190	-0.6757	<0.001[b]	3	100	NA
Erlotinib	-0.6756	<0.001[b]	3	100	EGFR inhibitor
BRD-K53120552	-0.6755	<0.001[b]	3	100	NA
BRD-K23021002	-0.6755	<0.001[b]	3	100	NA
Heptaminol	-0.6754	<0.001[b]	3	100	Vasoconstrictor

[a]P<0.01, [b]P<0.001. NA, not available.

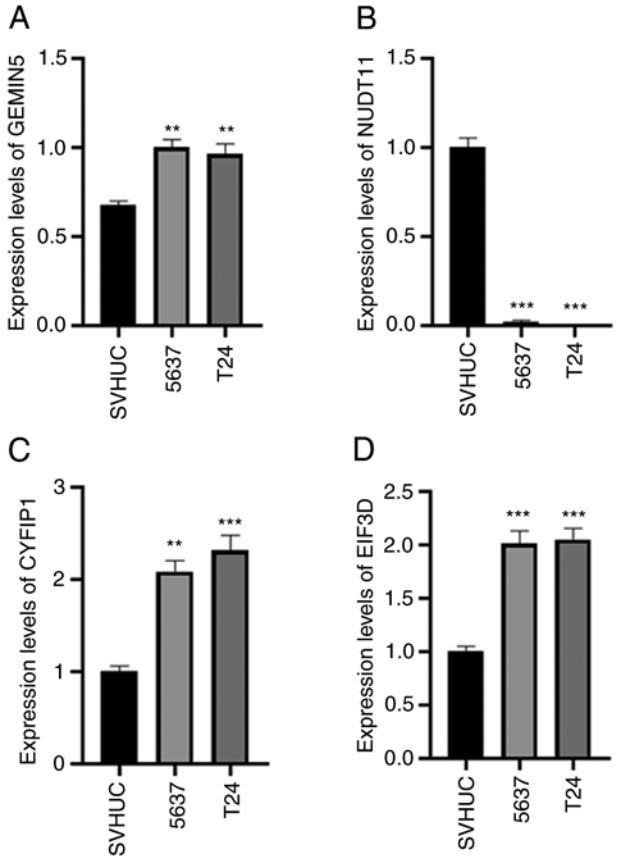

Figure 14. Results of reverse transcription-quantitative PCR analysis. Expression of (A) Gem nuclear organelle-associated protein 5; (B) Nudix hydrolase 11; (C) Cytoplasmic FMR1 interacting protein 1; and (D) Eukaryotic translation initiation factor 3 subunit D. **P<0.01, ***P<0.001 vs. control.

CYFIP1, and EIF3D), which were shown to be differentially expressed in bladder cancer cell lines based on RT-qPCR validation. Through KEGG and GO enrichment analyses, the potential biological functions of m7G-related genes in BLCA were explored. Cell experiments also demonstrated that the viability and proliferation of T24 and 5637 cells were significantly inhibited by knocking down GEMIN5. Next, the training set (TCGA cohort) was used to construct the predictive model, and the validation set (GEO cohort) was used to test the reliability of the model. The risk score calculated based on the four-gene model could forecast BLCA patient prognosis independently. Predictive nomograms that considered both clinicopathological features and risk scores were also built. Consequently, the risk signature reported on the present study could help clinicians make precise personalized survival predictions. Moreover, the current study found that m7G-related genes were closely associated with the immune microenvironment of BLCA, and immune infiltration in patients with BLCA could also be predicted based in the present risk model. Together, this prognostic model was strongly associated with clinicopathological factors, immune cells and immune-related functions.

As an essential regulator of m7G, GEMIN5 expression was found to be significantly upregulated in BLCA and associated with a poor patient prognosis. GEMIN5 can regulate translation, and has been reported to specifically bind the m7G cap (38). Other studies have shown that its expression is increased in gastric cancer tissue, acute myeloid leukemia, and liver cancer (17,39,40). Furthermore, GEMIN5 can exert oncogenic effects by regulating mRNA splicing and tumor cell motility, and by reprogramming cellular translation (41,42). CYFIP1 is a newly identified tumor suppressor. CYFIP1/2, WASF1/2/3, NCKAP1/1 L, Abi1/2/3, and BRK1 form a heteropentameric complex called the WASF regulatory complex (43). Abnormal distribution of CYFIP1 has been observed with cancer metastasis and invasion, and a previous study managed to inhibit breast cancer metastasis by blocking CYFIP1 and Rac1 protein interactions, actin polymerization, and β1-integrin/FAK/Src signaling (44). Moreover, a stapled peptide targeting NCKAP1 and CYFIP1 was designed to destabilize the WASF3 complex to inhibit invasion (45). NUDT11 is a phosphoinositide phosphohydrolase, and the turnover of bisphosphonates can affect cancer cell apoptosis (46). The present results suggested that NUDT11 was expressed at a lower level in BLCA than in normal tissue cells, but high levels of its expression implied a worse prognosis. A previous study showed that, when NUDT11 was suppressed, the proliferation and viability of prostate cancer cells were affected, and colony

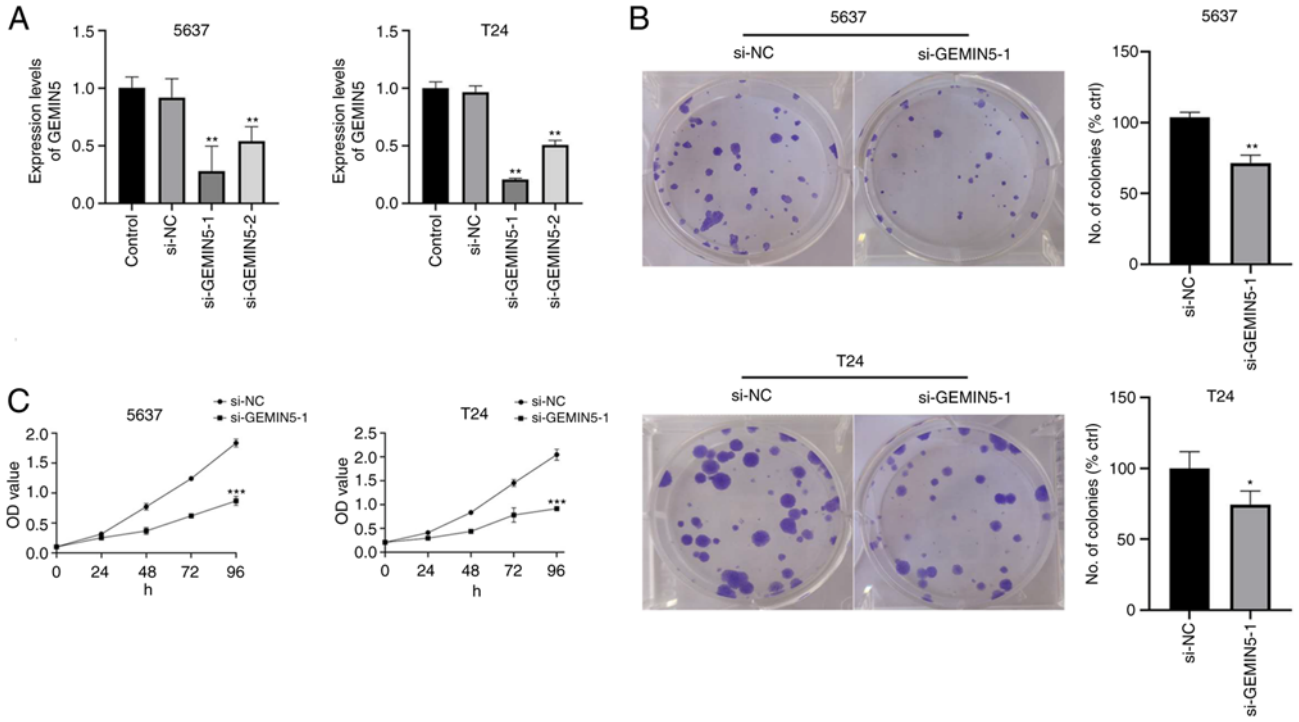

Figure 15. Effect of knockdown GEMIN5 on the proliferation of T24 and 5637 cells. (A) Expression of GEMIN5 after knockdown. (B) Colony formation assay to detect the influence of GEMIN5 on the proliferation of T24 and 5637 cells. (C) Cell Counting Kit-8 assay was used to detect the influence of GEMIN5 on the proliferation of T24 and 5637 cells. Data are shown as the mean ± SD. *P<0.05, **P<0.01, ***P<0.001 vs. negative control small interfering RNA. GEMIN5, gem nuclear organelle-associated protein 5.

formation was significantly reduced (47). EIF3 is the largest and most complex ribosomal EIF complex (48); it binds to the 40S ribosome and maintains the dissociation of the 40S and 60S ribosomal subunits. The function of EIF3 in promoting or inhibiting tumor progression is controversial. For example, EIF3D has been reported to promote colon cancer (49), melanoma (50), and breast cancer (51), but it is expressed at lower levels in liver cancer than in normal tissues. and is associated with a better prognosis (52). An examination of EIF3E mRNA levels in non-small cell lung carcinoma and breast cancer showed low levels in ~1/3 of the samples (53). However, the EIF3E levels in human glioblastoma cells were high, and siRNA-mediated knockdown inhibited cell proliferation (54). The present results suggested that EIF3D was a suppressor of BLCA, and that increased expression was associated with a better prognosis for patients. However, various claims about the association between the EIF3 subunit and cancer lack strength and appear to be based on experiments devoid of strict controls (55,56). Changes in EIF3 in other parts of the cell or in functions such as the activation of transcription factors or protein kinases can influence the status of cancer (57). In conclusion, the role of EIF3 is complex, and the same EIF3 subunit could have opposite roles in different cancer types. The biological processes associated with the effect of EIF3D on BLCA need to be further investigated.

Cancer immunity plays a key role in cancer progression, and increasing evidence suggests that the tumor immune microenvironment is vital for the initiation and progression of bladder cancer (10,58). Notably, the current results showed that, although immune cells such as CD8^{+} T cells markedly infiltrated BLCA, they did not appear to be effective in killing cancer cells in the high-risk group; instead, high levels of CD8^{+} T cell infiltration led to a worse prognosis. Immune functional analysis revealed that the high-risk group had higher levels of cancer-associated fibroblasts, which could produce fibrous cocoons to protect cancer cells. Excessive parainflammation can transform M1-type macrophages into M2-type macrophages, thus inhibiting immune functions and promoting tumor progression (59). Chemokines released by tumor cells can recruit T cells to reach the tumor tissue and be activated by tumor antigens. However, only 10% of T cells recruited to the tumor microenvironment can recognize tumor cells; the rest act as 'bystanders' and have no cytotoxic effect on tumor cells, such as exhausted T cells that express high levels of the immune checkpoint molecules PD-1, CTLA4, and TIGIT (60). A recent study defined tumor-derived lactate as an inhibitor of CD8^{+} T cell cytotoxicity (61). Therefore, in high-risk patients defined based on the aforementioned risk model, the tumor could have strong immune evasion abilities. Importantly, the present study found that immune checkpoint molecules were significantly expressed in the high-risk group, and immunotherapy may thus be effective for these patients. Designing anti-BLCA drugs against these targets could be one future approach. Moreover, the current study found 10 compounds and 9 drugs to potentially treat BLCA. However, the present study has certain limitations. As the study was based on information within public databases, real-world prospective cohort studies are required to validate the risk score formula. In addition, the differential expression and cancer-promoting ability of related genes were only verified through cellular experiments, and the biological mechanism underlying the effects of m7G-related RNAs in BLCA remains unclear. Detailed *in vitro* and *in vivo* experiments need to be performed

to explore the important functions of the aforementioned four genes with prognostic properties in BLCA.

In conclusion, the present study screened four genes related to patient prognosis based on the correlation between BLCA and m7G modification regulators, and a risk scoring model with good predictive accuracy was established. Moreover, the relationship between risk score and tumor immunity was evaluated, which provided new ideas and methods for the treatment of BLCA.

Acknowledgements

Not applicable.

Funding

No funding was received.

Availability of data and materials

Publicly available datasets were analyzed in the present study. These data can be found in the following URLs: The Cancer Genome Atlas database (https://portal.gdc.cancer.gov/) and Gene Expression Omnibus database (https://www.ncbi.nlm.nih.gov/geo/). The data used and/or generated in the present study are available from the corresponding author on reasonable request.

Authors' contributions

CZ, JX, and KH conceived and designed the experiments, and contributed reagents/materials/analysis tools. SZ, TZ, KH and JL made contributions to the methodology and statistical analysis, and provided supervision. CZ, JX, SZ, JL and TZ performed the data collection and analyzed the data. TZ and KH confirm the authenticity of all the raw data. CZ, JX, TZ and KH contributed to the writing of the manuscript. All authors read and approved the final manuscript.

Ethics approval and consent to participate

Not applicable.

Patient consent for publication

Not applicable.

Competing interests

The authors declare that they have no competing interests.

References

1. Richters A, Aben KKH and Kiemeney L: The global burden of urinary bladder cancer: An update. World J Urol 38: 1895-1904, 2020.
2. Zhu CZ, Ting HN, Ng KH and Ong TA: A review on the accuracy of bladder cancer detection methods. J Cancer 10: 4038-4044, 2019.
3. Cathomas R, Lorch A, Bruins HM, Compérat EM, Cowan NC, Efstathiou JA, Fietkau R, Gakis G, Hernández V, Espinós EL, *et al*: The 2021 updated European association of urology guidelines on metastatic urothelial carcinoma. Eur Urol 81: 95-103, 2022.
4. Kanehisa M and Bork P: Bioinformatics in the post-sequence era. Nat Genet 33 (Suppl): S305-S310, 2003.
5. Foulkes AC, Watson DS, Griffiths CEM, Warren RB, Huber W and Barnes MR: Research techniques made simple: Bioinformatics for genome-scale biology. J Invest Dermatol 137: e163-e168, 2017.
6. Zafeiris D, Rutella S and Ball GR: An artificial neural network integrated pipeline for biomarker discovery using Alzheimer's disease as a case study. Comput Struct Biotechnol J 16: 77-87, 2018.
7. Xie R, Xie M, Zhu L, Chiu JWY, Lam W and Yap DYH: The relationship of pyroptosis-related genes, patient outcomes, and tumor-infiltrating cells in bladder urothelial carcinoma (BLCA). Front Pharmacol 13: 930951, 2022.
8. Xu C, Song L, Peng H, Yang Y, Liu Y, Pei D, Guo J, Liu N, Liu J, Li X, *et al*: Clinical eosinophil-associated genes can serve as a reliable predictor of bladder urothelial cancer. Front Mol Biosci 9: 963455, 2022.
9. Jin K, Qiu S, Jin D, Zhou X, Zheng X, Li J, Liao X, Yang L and Wei Q: Development of prognostic signature based on immune-related genes in muscle-invasive bladder cancer: Bioinformatics analysis of TCGA database. Aging (Albany NY) 13: 1859-1871, 2021.
10. Chen X, Xu R, He D, Zhang Y, Chen H, Zhu Y, Cheng Y, Liu R, Zhu R, Gong L, *et al*: CD8(+) T effector and immune checkpoint signatures predict prognosis and responsiveness to immunotherapy in bladder cancer. Oncogene 40: 6223-6234, 2021.
11. Liu Z, Tang Q, Qi T, Othmane B, Yang Z, Chen J, Hu J and Zu X: A robust hypoxia risk score predicts the clinical outcomes and tumor microenvironment immune characters in bladder cancer. Front Immunol 12: 725223, 2021.
12. Olkhov-Mitsel E, Hodgson A, Liu SK, Vesprini D, Bayani J, Bartlett JMS, Xu B and Downes MR: Upregulation of IFNγ-mediated chemokines dominate the immune transcriptome of muscle-invasive urothelial carcinoma. Sci Rep 12: 716, 2022.
13. Boccaletto P, Magnus M, Almeida C, Zyla A, Astha A, Pluta R, Baginski B, Jankowska E, Dunin-Horkawicz S, Wirecki TK, *et al*: RNArchitecture: A database and a classification system of RNA families, with a focus on structural information. Nucleic Acids Res 46: D202-D205, 2018.
14. Jühling F, Mörl M, Hartmann RK, Sprinzl M, Stadler PF and Pütz J: tRNAdb 2009: Compilation of tRNA sequences and tRNA genes. Nucleic Acids Res 37: D159-D162, 2009.
15. Edmonds CG, Crain PF, Gupta R, Hashizume T, Hocart CH, Kowalak JA, Pomerantz SC, Stetter KO and McCloskey JA: Posttranscriptional modification of tRNA in thermophilic archaea (Archaebacteria). J Bacteriol 173: 3138-3148, 1991.
16. Luo Y, Yao Y, Wu P, Zi X, Sun N and He J: The potential role of N(7)-methylguanosine (m7G) in cancer. J Hematol Oncol 15: 63, 2022.
17. Li XY, Wang SL, Chen DH, Liu H, You JX, Su LX and Yang XT: Construction and validation of a m7G-related gene-based prognostic model for gastric cancer. Front Oncol 12: 861412, 2022.
18. Tomikawa C: 7-methylguanosine modifications in transfer RNA (tRNA). Int J Mol Sci 19: 4080, 2018.
19. Yang Z, Zhang S, Xia T, Fan Y, Shan Y, Zhang K, Xiong J, Gu M and You B: RNA modifications meet tumors. Cancer Manag Res 14: 3223-3243, 2022.
20. Rong D, Sun G, Wu F, Cheng Y, Sun G, Jiang W, Li X, Zhong Y, Wu L, Zhang C, *et al*: Epigenetics: Roles and therapeutic implications of non-coding RNA modifications in human cancers. Mol Ther Nucleic Acids 25: 67-82, 2021.
21. Zhang M, Song J, Yuan W, Zhang W and Sun Z: Roles of RNA methylation on tumor immunity and clinical implications. Front Immunol 12: 641507, 2021.
22. Furuichi Y: Discovery of m(7)G-cap in eukaryotic mRNAs. Proc Jpn Acad Ser B Phys Biol Sci 91: 394-409, 2015.
23. Reddy R, Singh R and Shimba S: Methylated cap structures in eukaryotic RNAs: Structure, synthesis and functions. Pharmacol Ther 54: 249-267, 1992.
24. R Core Team: R: A language and environment for statistical computing. R Foundation for Statistical Computing, Vienna, 2012. http://www.R-project.org/.
25. Szklarczyk D, Gable AL, Lyon D, Junge A, Wyder S, Huerta-Cepas J, Simonovic M, Doncheva NT, Morris JH, Bork P, *et al*: STRING v11: Protein-protein association networks with increased coverage, supporting functional discovery in genome-wide experimental datasets. Nucleic Acids Res 47: D607-D613, 2019.

26. Tang Z, Li C, Kang B, Gao G, Li C and Zhang Z: GEPIA: A web server for cancer and normal gene expression profiling and interactive analyses. Nucleic Acids Res 45: W98-W102, 2017.
27. Li T, Fan J, Wang B, Traugh N, Chen Q, Liu JS, Li B and Liu XS: TIMER: A web server for comprehensive analysis of tumor-infiltrating immune cells. Cancer Res 77: e108-e110, 2017.
28. Geeleher P, Cox N and Huang RS: pRRophetic: An R package for prediction of clinical chemotherapeutic response from tumor gene expression levels. PLoS One 9: e107468, 2014.
29. Livak KJ and Schmittgen TD: Analysis of relative gene expression data using real-time quantitative PCR and the 2(-Delta Delta C(T)) method. Methods 25: 402-408, 2001.
30. Lai H, Cheng X, Liu Q, Luo W, Liu M, Zhang M, Miao J, Ji Z, Lin GN, Song W, *et al*: Single-cell RNA sequencing reveals the epithelial cell heterogeneity and invasive subpopulation in human bladder cancer. Int J Cancer 149: 2099-2115, 2021.
31. Huang Z, Yan Y, Wang T, Wang Z, Cai J, Cao X, Yang C, Zhang F, Wu G and Shen B: Identification of ENO1 as a prognostic biomarker and molecular target among ENOs in bladder cancer. J Transl Med 20: 315, 2022.
32. Liu J, Zhou Z, Jiang Y, Lin Y, Yang Y, Tian C, Liu J, Lin H and Huang B: EPHA3 could be a novel prognosis biomarker and correlates with immune infiltrates in bladder cancer. Cancers (Basel) 15: 621,2023.
33. Yu X, Luo B, Lin J and Zhu Y: Alternative splicing event associated with immunological features in bladder cancer. Front Oncol 12: 966088, 2023.
34. Chen Z, Zhu W, Zhu S, Sun K, Liao J, Liu H, Dai Z, Han H, Ren X, Yang Q, *et al*: METTL1 promotes hepatocarcinogenesis via m(7) G tRNA modification-dependent translation control. Clin Transl Med 11: e661, 2021.
35. Zhu J, Liu X, Chen W, Liao Y, Liu J, Yuan L, Ruan J and He J: Association of RNA m7G modification gene polymorphisms with pediatric glioma risk. Biomed Res Int 2023: 3678327, 2023.
36. Han H, Yang C, Ma J, Zhang S, Zheng S, Ling R, Sun K, Guo S, Huang B and Liang Y: N(7)-methylguanosine tRNA modification promotes esophageal squamous cell carcinoma tumorigenesis via the RPTOR/ULK1/autophagy axis. Nat Commun 13: 1478, 2022.
37. Xia P, Zhang H, Xu K, Jiang X, Gao M, Wang G, Liu Y, Yao Y, Chen X, Ma W, *et al*: MYC-targeted WDR4 promotes proliferation, metastasis, and sorafenib resistance by inducing CCNB1 translation in hepatocellular carcinoma. Cell Death Dis 12: 691, 2021.
38. Xu C, Ishikawa H, Izumikawa K, Li L, He H, Nobe Y, Yamauchi Y, Shahjee HM, Wu XH, Yu YT, *et al*: Structural insights into Gemin5-guided selection of pre-snRNAs for snRNP assembly. Genes Dev 30: 2376-2390, 2016.
39. Li XY, Zhao ZJ, Wang JB, Shao YH, Hui-Liu, You JX and Yang XT: m7G methylation-related genes as biomarkers for predicting overall survival outcomes for hepatocellular carcinoma. Front Bioeng Biotechnol 10: 849756, 2022.
40. Shao J, Wang S, West-Szymanski D, Karpus J, Shah S, Ganguly S, Smith J, Zu Y, He C, Li Z, *et al*: Cell-free DNA 5-hydroxymethylcytosine is an emerging marker of acute myeloid leukemia. Sci Rep 12: 12410, 2022.
41. Lee JH, Horak CE, Khanna C, Meng Z, Yu LR, Veenstra TD and Steeg PS: Alterations in Gemin5 expression contribute to alternative mRNA splicing patterns and tumor cell motility. Cancer Res 68: 639-644, 2008.
42. Wollen KL, Hagen L, Vågbø CB, Rabe R, Iveland TS, Aas PA, Sharma A, Sporsheim B, Erlandsen HO, Palibrk V, *et al*: ALKBH3 partner ASCC3 mediates P-body formation and selective clearance of MMS-induced 1-methyladenosine and 3-methylcytosine from mRNA. J Transl Med 19: 287, 2021.
43. Limaye AJ, Whittaker MK, Bendzunas GN, Cowell JK and Kennedy EJ: Targeting the WASF3 complex to suppress metastasis. Pharmacol Res 182: 106302, 2022.
44. Chang JW, Kuo WH, Lin CM, Chen WL, Chan SH, Chiu MF, Chang IS, Jiang SS, Tsai FY, Chen CH, *et al*: Wild-type p53 upregulates an early onset breast cancer-associated gene GAS7 to suppress metastasis via GAS7-CYFIP1-mediated signaling pathway. Oncogene 37: 4137-4150, 2018.
45. Teng Y, Qin H, Bahassan A, Bendzunas NG, Kennedy EJ and Cowell JK: The WASF3-NCKAP1-CYFIP1 complex is essential for breast cancer metastasis. Cancer Res 76: 5133-5142, 2016.
46. Morrison BH, Bauer JA, Kalvakolanu DV and Lindner DJ: Inositol hexakisphosphate kinase 2 mediates growth suppressive and apoptotic effects of interferon-beta in ovarian carcinoma cells. J Biol Chem 276: 24965-24970, 2001.
47. Grisanzio C, Werner L, Takeda D, Awoyemi BC, Pomerantz MM, Yamada H, Sooriakumaran P, Robinson BD, Leung R, Schinzel AC, *et al*: Genetic and functional analyses implicate the NUDT11, HNF1B, and SLC22A3 genes in prostate cancer pathogenesis. Proc Natl Acad Sci U S A 109: 11252-11257, 2012.
48. Bandyopadhyay A, Lakshmanan V, Matsumoto T, Chang EC and Maitra U: Moe1 and spInt6, the fission yeast homologues of mammalian translation initiation factor 3 subunits p66 (eIF3d) and p48 (eIF3e), respectively, are required for stable association of eIF3 subunits. J Biol Chem 277: 2360-2367, 2002.
49. Yu X, Zheng B and Chai R: Lentivirus-mediated knockdown of eukaryotic translation initiation factor 3 subunit D inhibits proliferation of HCT116 colon cancer cells. Biosci Rep 34: e00161, 2014.
50. Sudo H, Tsuji AB, Sugyo A, Kohda M, Sogawa C, Yoshida C, Harada YN, Hino O and Saga T: Knockdown of COPA, identified by loss-of-function screen, induces apoptosis and suppresses tumor growth in mesothelioma mouse model. Genomics 95: 210-216, 2010.
51. Fan Y and Guo Y: Knockdown of eIF3D inhibits breast cancer cell proliferation and invasion through suppressing the Wnt/β-catenin signaling pathway. Int J Clin Exp Pathol 8: 10420-10427, 2015.
52. Golob-Schwarzl N, Krassnig S, Toeglhofer AM, Park YN, Gogg-Kamerer M, Vierlinger K, Schröder F, Rhee H, Schicho R, Fickert P and Haybaeck J: New liver cancer biomarkers: PI3K/AKT/mTOR pathway members and eukaryotic translation initiation factors. Eur J Cancer 83: 56-70, 2017.
53. Hershey JW: The role of eIF3 and its individual subunits in cancer. Biochim Biophys Acta 1849: 792-800, 2015.
54. Sesen J, Cammas A, Scotland SJ, Elefterion B, Lemarié A, Millevoi S, Mathew LK, Seva C, Toulas C, Moyal ECJ and Skuli N: Int6/eIF3e is essential for proliferation and survival of human glioblastoma cells. Int J Mol Sci 15: 2172-2190, 2014.
55. Feng X, Li J and Liu P: The biological roles of translation initiation factor 3b. Int J Biol Sci 14: 1630-1635, 2018.
56. Wolf DA, Lin Y, Duan H and Cheng Y: eIF-Three to Tango: Emerging functions of translation initiation factor eIF3 in protein synthesis and disease. J Mol Cell Biol 12: 403-409, 2020.
57. Yin Y, Long J, Sun Y, Li H, Jiang E, Zeng C and Zhu W: The function and clinical significance of eIF3 in cancer. Gene 673: 130-133, 2018.
58. Luo Y, Chen L, Zhou Q, Xiong Y, Wang G, Liu X, Xiao Y, Ju L and Wang X: Identification of a prognostic gene signature based on an immunogenomic landscape analysis of bladder cancer. J Cell Mol Med 24: 13370-13382, 2020.
59. Undi RB, Filiberti A, Ali N and Huycke MM: Cellular carcinogenesis: Role of polarized macrophages in cancer initiation. Cancers (Basel) 14: 2811, 2022.
60. Scheper W, Kelderman S, Fanchi LF, Linnemann C, Bendle G, de Rooij MAJ, Hirt C, Mezzadra R, Slagter M, Dijkstra K, *et al*: Low and variable tumor reactivity of the intratumoral TCR repertoire in human cancers. Nat Med 25: 89-94, 2019.
61. Elia I, Rowe JH, Johnson S, Joshi S, Notarangelo G, Kurmi K, Weiss S, Freeman GJ, Sharpe AH and Haigi MC: Tumor cells dictate anti-tumor immune responses by altering pyruvate utilization and succinate signaling in CD8(+) T cells. Cell Metab 34: 1137-1150.e1136, 2022.